Biochemical Journal (2020) **477** 3583–3598
https://doi.org/10.1042/BCJ20200427

Research Article

RORα phosphorylation by casein kinase 1α as glucose signal to regulate estrogen sulfation in human liver cells

Hao Hu and Masahiko Negishi

Pharmacogenetics, Reproductive and Developmental Biology Laboratory, National Institute of Environmental Health Sciences, National Institutes of Health, Research Triangle Park, North Carolina 27709, U.S.A.

Correspondence: Masahiko Negishi (negishi@niehs.nih.gov)

Estrogen sulfotransferase (SULT1E1) metabolically inactivates estrogen and SULT1E1 expression is tightly regulated by multiple nuclear receptors. Human fetal, but not adult, livers express appreciable amounts of SULT1E1 protein, which is mimicked in human hepatoma-derived HepG2 cells cultured in high glucose (450 mg/dl) medium. Here, we have investigated this glucose signal that leads to phosphorylation of nuclear receptor RORα (NR1F1) at Ser100 and the transcription mechanism by which phosphorylated RORα transduces this signal to nuclear receptor HNF4α, activating the *SULT1E1* promoter. The promoter is repressed by non-phosphorylated RORα which binds a distal enhancer (−943/−922 bp) and interacts with and represses HNF4α-mediated transcription. In response to high glucose, RORα becomes phosphorylated at Ser100 and reverses its repression of HNF4α promoter activation. Moreover, the casein kinase CK1α, which is identified in an enhancer-bound nuclear protein complex, phosphorylates Ser100 in *in vitro* kinase assays. During these dynamic processes, both RORα and HNF4α remain on the enhancer. Thus, RORα utilizes phosphorylation to integrate HNF4α and transduces the glucose signal to regulate the *SULT1E1* gene in HepG2 cells and this phosphorylation-mediated mechanism may also regulate SULT1E1 expressions in the human liver.

Introduction

Estrogen is metabolically inactivated by sulfation and estrogen sulfotransferase (SULT1E1) specifically and efficiently (Km ~ 4 nM) catalyzes this reaction [1]. SULT1E1 is a member of the cytosolic sulfotransferase (SULT) family of enzymes that collectively sulfate numerous endobiotics and xenobiotics by transferring the sulfate group from 3′-phosphoadenosine 5′-phosphosulfate [2,3]. The expression of SULT1E1 is tightly regulated in tissues and organs differently to regulate metabolic balances of estrogen. In the liver, SULT1E1 is barely expressed in normal mice but highly induced in diabetic mice such as *db/db* mice [4]. SULT1E1 is also induced by treatments with therapeutics such as phenobarbital [5]. In human hepatoma-derived HepG2 cells, SULT1E1 is highly expressed when cells are cultured in medium containing high glucose concentrations [6]. Whereas these observations indicate that SULT1E1 may be involved in interplays between estrogen, glucose and diabetes, the cellular and molecular regulation of SULT1E1 expression is not understood well.

Sult1e1 cDNA first cloned from mouse testis was utilized to demonstrate induced expression of *Sult1e1* mRNA in the liver of diabetogenic *db/db* mice [4]. Genetic aberrations in *Sult1e1* improved anti-inflammatory responses and metabolic dysfunction in the liver of *ob/ob* female mice [7]. This suggests that SULT1E1 regulates estrogen's anti-inflammatory function by altering hepatic levels of active estrogen via sulfation. On the other hand, hepatic SULT1E1 is highly induced in inflammatory-related disease conditions such as sepsis, a deteriorating disease prognosis [8,9].

Received: 27 May 2020
Revised: 16 July 2020
Accepted: 20 July 2020

Accepted Manuscript online: 20 July 2020
Version of Record published: 28 September 2020

Biochemical Journal (2020) 477 3583–3598
https://doi.org/10.1042/BCJ20200427

Therefore, by regulating levels of active estrogen, SULT1E1 can become either a beneficial or detrimental factor in disease developments and a target of clinical treatments. For these notions, it is fundamental for us to understand the molecular basis of SULT1E1 expression.

SULT1E1 is expressed in fetal livers and repressed in adult livers of humans [10] as well as in human primary hepatocyte cultures [11]. The elevated SULT1E1 expression phenotype is modeled in human hepatoma-derived HepG2 cells [6] when cells are cultured in a DMEM medium that contains high glucose concentration (450 mg/dl). Consistent with this high expression, the promoter of the human *SULT1E1* gene is highly activated in HepG2 cells. This promoter contains a DR1 motif within the 100 bp distal enhancer (−1000/−901 bp), to which nuclear receptor HNF4α binds and loops the enhancer closely to a proximal region of the promoter to activate it [6]. Therefore, HepG2 cells may be a useful experimental model to investigate the glucose response mechanism of SULT1E1 expression.

In addition to HNF4α, various other nuclear receptors are independently reported to regulate hepatic SULT1E1 expression, which include glucocorticoid receptor (GR), liver X receptor (LXR), constitutive active/androstane receptor (CAR), pregnane X receptor (PXR), farnesoid X receptor (FXR) and retinoid-related orphan receptor α (RORα) [5,6,12–16]. Among these nuclear receptors, RORα is unique in its function to co-activate CAR in mouse livers [5]. In response to phenobarbital, RORα interacts with CAR on the *Sult1e1* promoter and undergoes phosphorylation at Ser100. Phosphorylated RORα co-activates CAR-mediated transcription of the promoter. These observations suggest that this inducible phosphorylation enables RORα to co-regulate other nuclear receptors. Therefore, we selected RORα as a possible candidate for regulating HNF4α on the 100 bp enhancer of the *SULT1E1* promoter in HepG2 cells and examined whether Ser100 is phosphorylated in response to glucose, allowing phosphorylated RORα to co-activate HNF4α.

In this manuscript, a phosphor-Ser100 peptide antibody was used to detect phosphorylated RORα. A 22 bp sequence overlapping DR1 and RORE (−943/−922 bp) was delineated from the 100 bp enhancer of the *SULT1E1* promoter and analyzed by cell-based reporter and gel-shift assays. Co-immunoprecipitation assays examined interactions between RORα and HNF4α. Chromatin immunoprecipitation and chromatin conformation capture assays were employed to examine bindings of nuclear receptors in response to glucose concentrations. The 22 bp DNA oligonucleotide was used in affinity chromatography to purify nuclear proteins for subsequent mass spectroscopic analysis and identify candidate protein kinases that might phosphorylate RORα. Experimental evidence will be presented to demonstrate that RORα bound to RORE is phosphorylated at Ser100 by casein kinase 1α in response to high glucose concentrations, interacting with HNF4α and co-activating the *SULT1E1* promoter. Subsequently, a novel concept that nuclear receptors integrate their function through phosphorylation to regulate genes will be discussed.

Materials and methods

Chemicals, antibodies, plasmids and primers and siRNAs

Common chemicals, HRP conjugated anti-GFP, anti-M2 Flag, anti-V5 His antibodies and anti-Flag M2 affinity agarose gel were from Sigma–Aldrich; media, supplements, reagents and primers (Supplementary Table S2) were from Thermo Fisher Scientific; ATP [γ-^{32}P] and [^{35}S] phosphor-adenosine phosphosulfate (PAPS) were from PerkinElmer; media and reagents were from Thermo Fisher Scientific; anti-phosphor Serine 100 of RORα and anti-RORα antibodies were from GenScript; antibodies against HNF4α (H171 and H1), β-actin (C4) and goat anti-rabbit or mouse HRP conjugated IgGs were from Santa Cruz Biotechnology; anti-human SULT1E1 antibody was from Proteintech; anti-CK1α and anti-RACK7 antibodies were from Novus Biologicals and Bethyl Laboratories, respectively; normal mouse and rabbit IgGs were from Cell Signaling Technology; anti-GFP sepharose beads were kindly provided by the protein expression core at NIHES; the −1081 bp human *SULT1E1* promoter (-1081-*SULT1E1*) and the *SULT1E1* construct containing a 175 bp *SULT1E1* enhancer and a 105 bp *SULT1E1* promoter (Δ-1081-*SULT1E1*) were previously described [6]. Plasmids Flag-tagged pcDNA3.1-HNF4α WT; pEGFP-HNF4α WT; Flag-tagged pcDNA3.1 RORα WT, RORα S100A and RORα S100D; GST-tagged RORα WT and RORα S100A were previously described [17]. SMARTpool: ON-TARGETplus HNF4A siRNA (L-003406-00-0005) and RORA siRNA (L-003440-00-0005) were from Dharmacon.

Cell cultures, treatments and subcellular fractionations

Human liver hepatocellular carcinoma cells Huh7, HepG2 and monkey kidney Cos-1 cells were obtained from ATCC and cultured in standard DMEM medium. DMEM glucose-free media supplemented with different

concentrations of glucose were used for cell treatments. Cell viabilities of these treated cells were measured by using Cell Counting Kit-8 (Dojindo Laboratories). Cytosolic and nuclear proteins from cultured cells were prepared as described previously [6]. Buffer A (10 mM HEPES pH = 7.6, 10 mM KCl, 1.5 mM $MgCl_2$, 0.3% NP-40, protease inhibitors cocktail) was used to obtain cytosolic fractions. NE buffer (10% glycerol, 10 mM HEPES, 0.1 M KCl, 3 mM $MgCl_2$, 300 mM NaCl, 0.1 mM EDTA, 1 mM $NaVO_4$, protease inhibitors cocktail) was used to extract nuclear fractions.

siRNA knockdown and quantitative reverse transcription PCR

Lipofectamine RNAiMAX and siRNAs were used for knockdown experiments in Huh7 cells. Total cellular RNA was extracted from cells by using TRIzol reagent in accordance to the manufacturer's instructions. Extracted mRNAs were reverse transcribed to cDNAs by using High-Capacity cDNA Reverse Transcription Kit. TaqMan probes (Supplementary Table S2) and Taqman Master mix were applied to measure respective mRNA expressions. Relative mRNA expressions were compared with the β-actin housekeeping gene of the treated cells. Real-time PCR was performed by using CFX96^{TM} Real-time system (Bio-Rad Laboratories).

Estrogen sulfating activity assays

An amount of 20 μg of HepG2 cytosolic extract and [^{35}S] PAPS as a sulfate donor were mixed in the presence of 0.1 μM or 100 μM E2 in a final 25 μl reaction containing 50 mM HEPES-NaOH, pH = 7.0. Reactions were first incubated at 37°C for 30 min, followed by 95°C for 5 min to inactivate reactions. The [^{35}S] sulfated E2 in supernatants was separated by using TLC procedures with ethyl acetate/n-butanol (2:1 by volume) on Whatman silica gel plate (PGC Scientific) and was visualized on X-ray film, which was subsequently counted in the Beckman LS6500 scintillation counter for radioactivity.

Electrophoretic mobility shift assays

The probes containing the respective DR1 and RORE spanning from −943 to −922 bp upstream of the *SULT1E1* translation start site and a consensus RORE are listed in Supplementary Table S2. These probes were labeled with ATP [γ-^{32}P] by using a T4 polynucleotide kinase (NEB) and purified using Illustra MicroSpin G-25 Columns (GE Healthcare). Each probe was incubated with respective proteins, and/or antibodies in binding buffer (10 mM Tris–HCl, pH = 7.5, 50 mM NaCl, 0.5 mM DTT, 10% glycerol, 0.5 μg poly (dI-dC), 0.05% NP-40). The samples were separated by electrophoresis on a non-denaturing 4% polyacrylamide gel in running buffer (7 mM Tris–HCl, pH = 7.5, 3 mM NaAc, 1 mM EDTA). The radioactive signal was subsequently developed onto autoradiography film (Denville Scientific).

Site direct mutagenesis and reporter gene assays

A series of *SULT1E1* promoter mutants were generated by using pGL3/Δ-1081-*SULT1E1* as a template and respective primers (Supplementary Table S2) according to manufacturer's instructions (QuikChange Site-Directed Mutagenesis Kit, Agilent Technologies). Luciferase reporter gene assays were conducted by transfecting respective *SULT1E1* promoters together with HNF4α or RORα into Huh7 cells, respectively. Luciferase activities of the transfected cells were measured using the Dual-Luciferase Reporter Assay System (Promega).

Chromatin immunoprecipitation (ChIP) and co-immunoprecipitation (CoIP) assays

ChIP samples of the treated cells were prepared using ChIP-IT Express Chromatin Immunoprecipitation Kit (Active Motif) according to the manufacturer's instructions. Precipitated chromatins were then used as a template for quantitative and real-time PCRs with specific primers (Supplementary Table S2). GFP-tagged HNF4α was cotransfected with Flag-tagged RORα WT, RORα S100A or RORα S100D into Cos-1 cells, respectively. Nuclear fractions of the transfected cells were obtained, which were used in CoIP reactions. 50 μg of nuclear extract was diluted in 100 μl of IP buffer (20 mM Tris, pH = 7.4, 0.5 mM EDTA, 1% Triton-X100, 10% Glycerol, 500 mM NaCl, protease inhibitors cocktail), which was incubated with 10 μl of anti-GFP antibody conjugated sepharose beads for precipitating GFP-tagged HNF4α. The precipitated proteins and 10% of the total input samples were subjected to SDS–PAGE for western blotting with anti-Flag-M2 HRP conjugated or anti-GFP HRP conjugated antibody, respectively.

Biochemical Journal (2020) 477 3583–3598
https://doi.org/10.1042/BCJ20200427

In vitro phosphorylation assays and western blotting

Escherichia coli BL21 (DE3) (Agilent Technologies) bacteria expressed GST-hRORα WT and its alanine mutant GST-hRORα S100A which were then purified by glutathione sepharose 4B (GE Healthcare). An amount of 6 μg of each purified protein was incubated with or without 200 ng of GST-CK1α (Promega), respectively, in 30 μl of kinase buffer (40 mM Tris pH = 7.5, 20 mM $MgCl_2$, 0.1 mg/ml BSA, 50 μM DTT) and 200 μM ATP at 30°C for 30 min. Samples were denatured and subjected to SDS–PAGE for western blotting analysis with antibodies against phosphorylated RORα at Ser100 or RORα, respectively. The membrane was blocked in Tris-buffered saline containing 0.1% Tween 20 (TBS-T) and 5% non-fat milk for 1 h and probed with the relevant antibody overnight at 4°C. HRP-conjugated secondary antibody was reacted with the probed primary antibody after washing. Signal was developed by using Western Bright ECL or Sirius kit (Advansta).

Protein purification and mass spectrometry

HepG2 cells were seeded and exposed to low glucose or high glucose conditions for 48 h, respectively, followed by nuclear protein extractions. The 22 bp *SULT1E1* enhancer was repeated four times and was subcloned into pGL3-TK basic plasmid between KpnI and BglII. The 4× *SULT1E1* enhancer was amplified from the plasmid by using the primers (Supplementary Table S2) and purified by using a QIAquick gel extraction kit (QIAGEN). The purified DNAs were biotinylated by using DNA Polymerase I, Large (Klenow) Fragment (NEB), and immobilized to Dynabeads M-280 Streptavidin (Thermo Fisher Scientific) for enriching the associated gene regulatory complexes from the HepG2 cell nuclear extracts. Beads containing biotinylated DNAs were incubated with the nuclear extracts for 3 h. The DNA-protein complexes were washed by the NE buffer, then eluted by an elution buffer (5 mM Tris–HCl, pH = 7.5, 500 mM EDTA, 1 M NaCl), followed by mass spectroscopic analysis. A complete list of enriched factors was submitted to the ProteomeXchange Consortium via the PRIDE [18] partner repository with the dataset identifier PXD016385.

Chromosome conformation capture (3c) assays

3C assays were conducted as previously described with minor modifications [6]. 1.5×10^6 HepG2 cells were seeded and treated with low glucose or high glucose conditions for 48 h, respectively. These cells were fixed with formaldehyde [final 2% (v/v)] for 10 min. Cells were suspended in 2 ml lysis buffer (50 mM Tris pH = 7.5, 150 mM NaCl, 5 mM EDTA, 0.5% NP-40, 1% Triton X-100, protease inhibitors). Cell pellets were harvested and suspended in 600 μl restriction enzyme buffer 2.1 containing 0.3% SDS (w/v), which were incubated at 37°C for 1 h. Thereafter, Triton X-100 was added in the reaction to a final concentration of 2.1% (v/v), followed by incubation at 37°C for 1 h. The treated cells were digested by 600 U restriction enzyme BstYI (NEB) for 15 min at 60°C, then overnight at 37°C. The digested chromatins were ligated by 20 μl T4 DNA ligase (NEB) in a 7 ml reaction at 16°C overnight. Proteinase K, NaCl, and EDTA were added to the ligation mixtures to final concentrations of 40 μg/ml, 0.2 M and 1 mM, respectively for reverse cross-linking, 16 h at 65°C. RNase A was added to the mixtures to a final concentration of 40 μg/ml. The mixtures were incubated for 45 min at 37°C before purification by using a QIAquick PCR purification kit (QIAGEN). The purified DNAs were subjected to RT-PCR and quantitative PCR analysis of control and ligated fragments by respective primers (Supplementary Table S2).

Statistical analysis

Two group comparisons were analyzed by the student's *t*-test. Multiple group comparisons were analyzed with one-way or two-way analysis of variance (ANOVA) followed by the least significant difference post hoc test. Differences were considered significant when $P < 0.05$.

Results

SULT1E1 is induced at high glucose cultured HepG2 cells

DMEM media containing different concentrations of glucose were utilized to treat HepG2 cells for 48 h, respectively, followed by measuring *SULT1E1* and *STS* mRNA expression levels. Low glucose (40 mg/dl), normal glucose (140 mg/dl) and high glucose (450 mg/dl) were selected as they imitate hypoglycemia, normal and hyperglycemia conditions in humans, respectively [19,20]. *SULT1E1* mRNA expression in HepG2 cells was 114 times higher at high glucose condition than it was at low glucose condition (Figure 1A). No significant differences were observed between the normal glucose condition and high glucose condition. However, steroid sulfatase (STS), the enzyme that activates sulfated estrogen to estrogen, was significantly repressed in the high glucose condition (Figure 1B). Consistent with mRNA

Biochemical Journal (2020) **477** 3583–3598
https://doi.org/10.1042/BCJ20200427

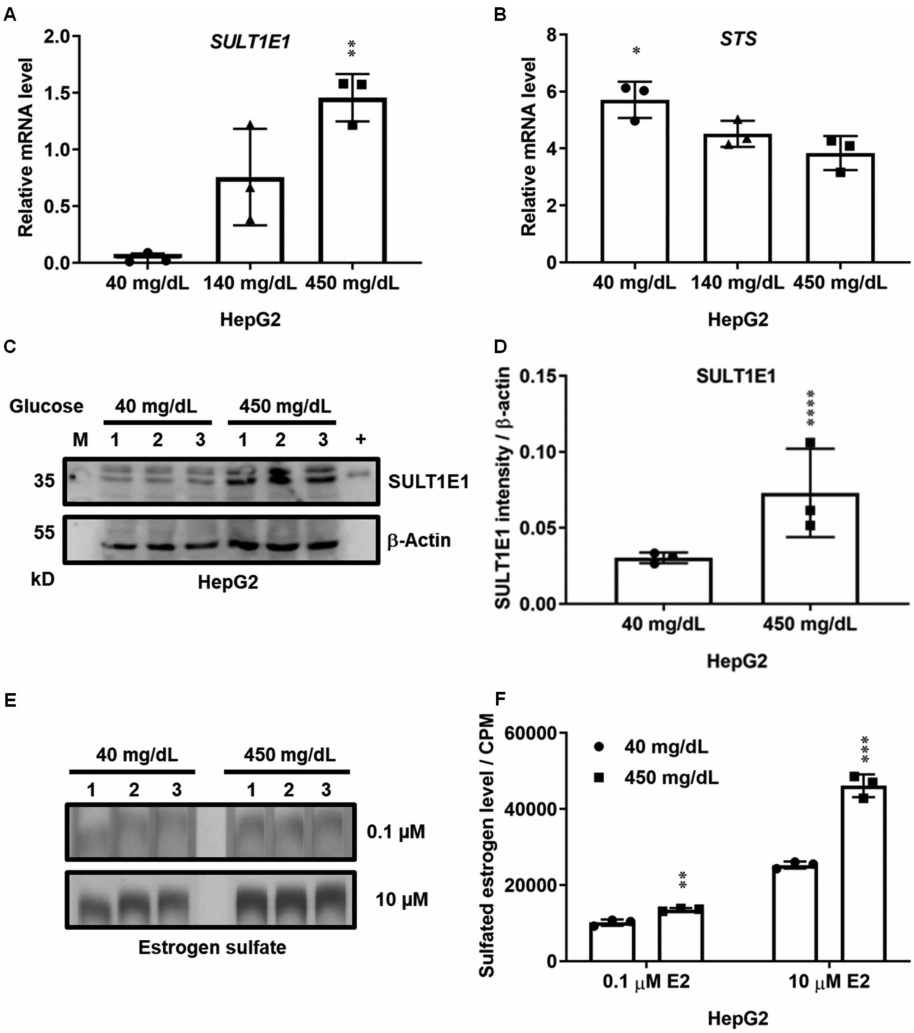

Figure 1. High glucose induces SULT1E1 expression in HepG2 cells.

Glucose-responsive (**A**) *SULT1E1* and (**B**) *STS* gene expressions were detected in HepG2 cells by qRT-PCR. The values ($N = 3$) represent means ± S.D. Mean difference is significant from low glucose treated group at ** $P < 0.005$; * $P < 0.05$ (One-way ANOVA). (**C**) SULT1E1 protein expressions in response to glucose exposures were measured in HepG2 cells by western blotting, followed by (**D**) densitometry analysis of the SULT1E1 band intensity. Experiments were conducted in triplicates. '+' indicates a bacterial expressed SULT1E1. (**E**) Estrogen sulfation was measured in both low glucose treated and high glucose treated HepG2 cells in the presence of 0.1 μM or 10 μM E2. (**F**) [^{35}S] sulfated E2 was separated by TLC procedures, followed by measuring their radioactivities. The values ($N = 3$) represent means ± S.D. Mean difference is significant from low glucose treated group at **** $P < 0.0001$; *** $P < 0.0005$; ** $P < 0.005$ (Student's *t*-test).

expression, SULT1E1 protein expression was significantly induced in high glucose cultured HepG2 cells (Figure 1C, D). Estrogen sulfation was significantly activated in high glucose treated HepG2 cells in the presence of both 0.1 μM and 10 μM E2 as substrate (Figure 1E,F). This induction of *SULT1E1* by high glucose was also observed in the HepG2 3D culture and Huh7 cells (Supplementary Figure S1A,B). Both low and high glucose exposures for HepG2 and Huh7 cells did not significantly affect their cell viabilities (Supplementary Figure S1C,D). These observations suggested that glucose exposures regulate *SULT1E1* gene expression in cells. The SULT1E1 activation and STS suppression at high glucose conditions may serve as a negative feedback loop to inactivate estrogens in human liver cells.

A HNF4α and RORα overlapping enhancer on the *SULT1E1* gene

To investigate how *SULT1E1* is regulated in cells, a detailed DNA sequence analysis of the *SULT1E1* promoter was performed by using the software MatInspector [21]. Intriguingly, a putative DR1 (HNF4α binding) and a

Biochemical Journal (2020) **477** 3583–3598
https://doi.org/10.1042/BCJ20200427

putative RORE (RORα binding) overlapping region was detected spanning from −943 to −922 bp upstream of *SULT1E1* translation start site (Figure 2A, boxed sequences). It was previously shown that HNF4α binds to the DR1 element of the *SULT1E1* gene, looping a 100 bp *SULT1E1* enhancer (Figure 2A) to its proximal promoter thereby activating gene expression [6]. However, the role of the putative RORE within the *SULT1E1* enhancer in the regulation of gene expression remains unclear. To decipher the possible bindings of HNF4α and RORα to the *SULT1E1* enhancer, two probes that represent the DR1 containing RORE half-site (DR1, solid line) and the RORE containing DR1 half-site (RORE, dashed line) were utilized in gel shift assays. Incubating the DR1 probe with a HepG2 nuclear extract resulted in the formation of two complexes, which are indicated by a solid arrow (upper) and blank arrow (lower), respectively (Figure 2B, lane 2). However, the predominant complex was the upper complex. Both complexes were supershifted by an antibody against HNF4α (Figure 2B, lane 3, dashed arrow), suggesting the binding of HNF4α to the DR1 probe. The antibody against RORα significantly weakened the binding for the upper complex and shifted the binding of the lower complex (Figure 2B, lane 4), indicating a possible interaction between HNF4α and RORα and a weak binding of RORα to the DR1 probe. Similarly, the same complexes were formed when incubating the RORE probe with a HepG2 nuclear extract, whereas the major complex was the lower complex (Figure 2B, lane 7). The complexes were supershifted by both anti-HNF4α antibody (Figure 2B, lane 8) and anti-RORα antibody (Figure 2B, lane 9), respectively, which suggested RORα binding and a possible interaction between RORα and HNF4α on the RORE probe. The consensus RORE which is known for RORα binding was used as a positive control to validate the quality of the assays (Figure 2B, lanes 11–14). These observations indicated a HNF4α and RORα binding complex on the *SULT1E1* enhancer.

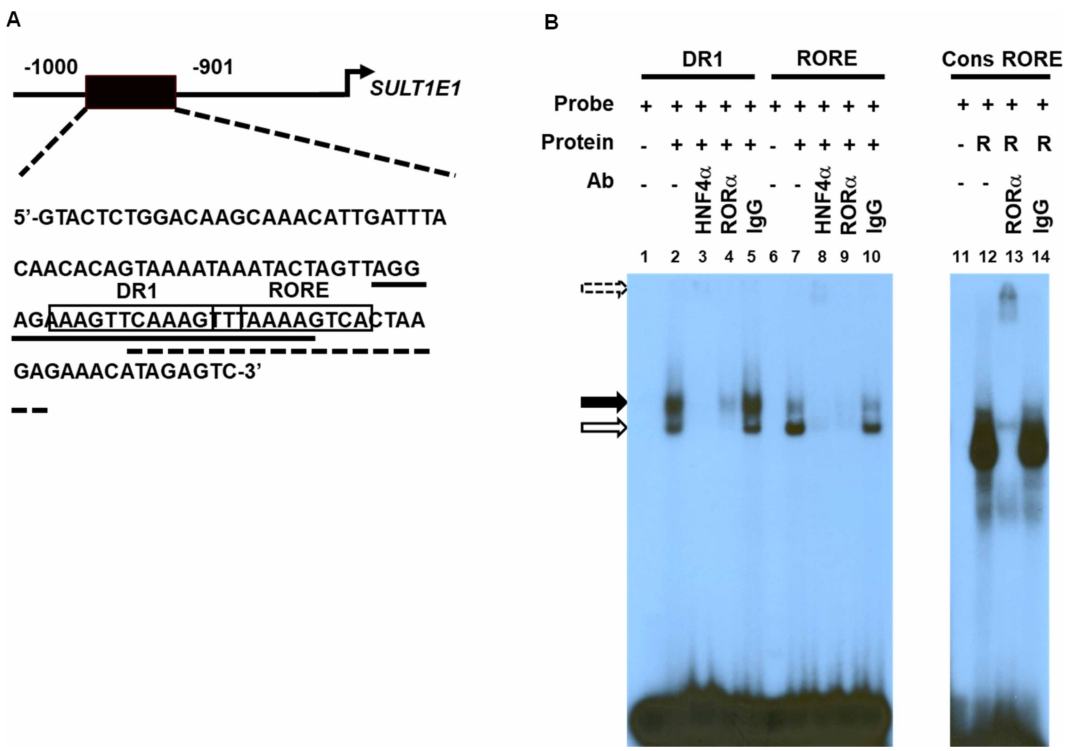

Figure 2. Nuclear receptors HNF4α and RORα bind to the *SULT1E1* gene.

(**A**) Schematic representation of the HNF4α (DR1) and RORα (RORE) binding elements on the *SULT1E1* gene. A DR1 and RORE overlapping region (boxed sequences) was detected ∼1000 bp upstream of the *SULT1E1* promoter. The *SULT1E1* DR1 containing RORE half-site (solid line), and the *SULT1E1* RORE containing DR1 half-site (dashed line) were used as probes in the gel shift assays. (**B**) Bindings of HNF4α and RORα to the *SULT1E1* gene. The probes were radioactively labeled, which were incubated with a HepG2 nuclear extract or an *in vitro* translated RORα (R), respectively. The antibodies against HNF4α and RORα were used to supershift (dashed arrow) the formed protein/DNA binding complexes (solid and blank arrows). A normal IgG was used as a negative control for the antibodies used in the study. The Cons RORE was served as a positive control of the assays. Experiments were repeated three times.

Biochemical Journal (2020) **477** 3583–3598
https://doi.org/10.1042/BCJ20200427

HNF4α and RORα cooperatively regulate *SULT1E1* promoter

To characterize the roles of HNF4α and RORα in regulating *SULT1E1* promoter activities, a −1081 bp *SULT1E1*-Luc reporter, an 800 bp internal deleted Δ-1081 bp *SULT1E1*-Luc reporter containing the 22 bp enhancer and the 105 bp proximal promoter, and their respective mutants on DR1 or/and RORE were constructed (Figure 3A). They were transfected into Huh7 cells for reporter gene assays. First, the internal deletion of the *SULT1E1* promoter increased its promoter activity about seven times compared with the full-length

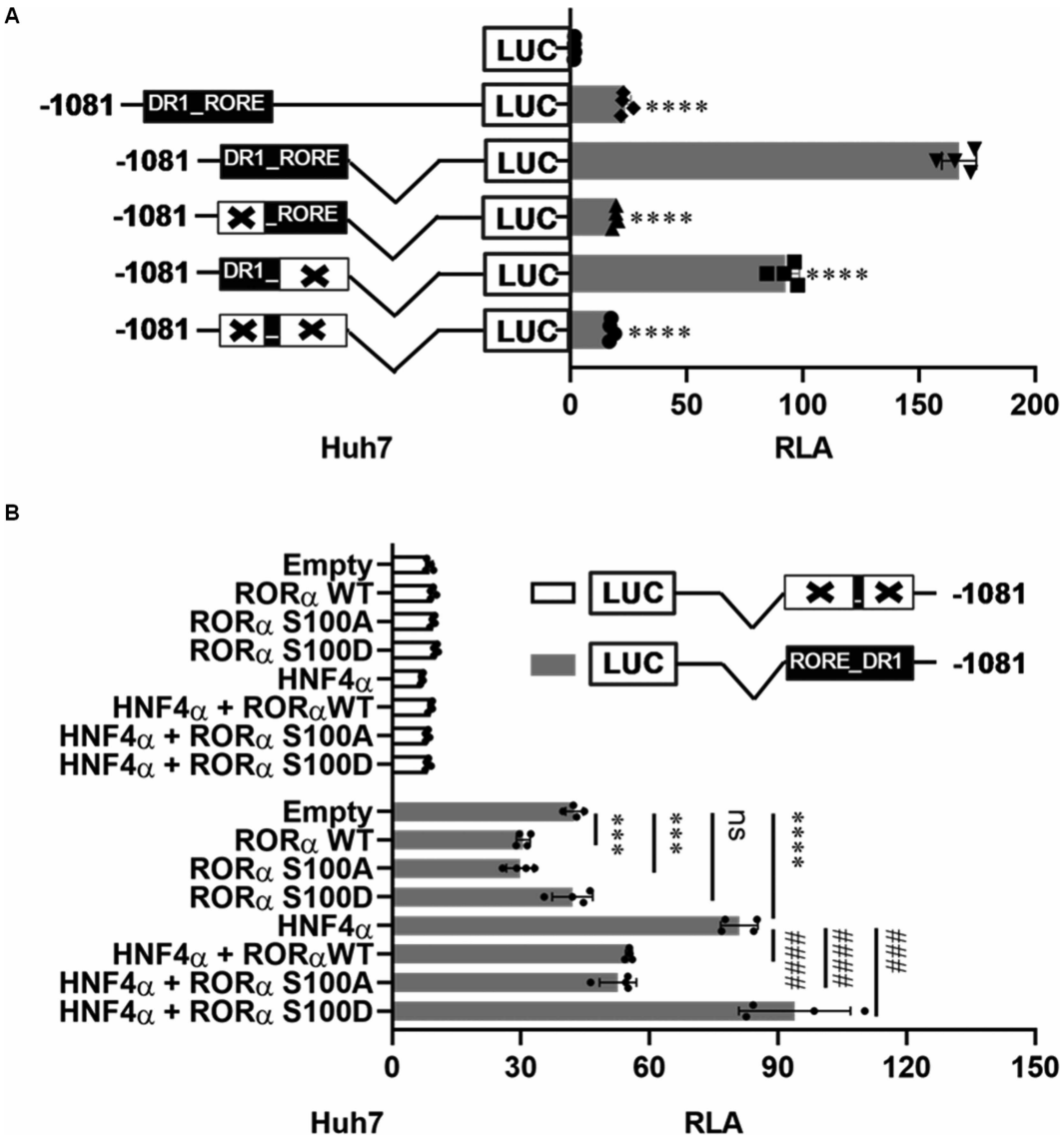

Figure 3. Nuclear receptors HNF4α and RORα cooperatively regulate *SULT1E1* via a 22 bp enhancer.

(**A**) Role of the 22 bp enhancer in regulating *SULT1E1* promoter. -1081 *SULT1E1*-Luc, Δ-1081 *SULT1E1*-Luc or its mutants was transfected into Huh7 cells, respectively for 24 h. Luciferase activities of the transfected cells were measured, which were normalized by Renilla luciferase (transfection control) activities. The values ($N = 4$) represent means ± S.D. Mean difference is significant from Δ-1081 *SULT1E1*-Luc transfected group at **** $P < 0.0001$ (One-way ANOVA). (**B**) Roles of HNF4α and RORα in regulating *SULT1E1* promoter. HNF4α and Δ-1081 *SULT1E1*-Luc or mutated Δ-1081 *SULT1E1*-Luc were cotransfected with RORα WT, RORα S100A or RORα S100D into Huh7 cells, respectively for 24 h. Luciferase activities of the transfected cells were measured, which were normalized by Renilla luciferase activities. The values ($N = 4$) represent means ± S.D. Mean difference is significant from empty vector transfected group at **** $P < 0.0001$; *** $P < 0.0005$; and from HNF4α transfected group at #### $P < 0.0001$; ### $P < 0.0005$ (Two-way ANOVA).

Biochemical Journal (2020) 477 3583–3598
https://doi.org/10.1042/BCJ20200427

promoter, confirming that the internal deletion facilitates the looping between the enhancer and the promoter thereby activating its promoter activity (Figure 3A). Mutating the DR1 and RORE individually or in combination dramatically decreased promoter activity, illustrating critical roles of the DR1 and RORE in supporting *SULT1E1* promoter activity (Figure 3A). To investigate whether HNF4α, RORα and its mutants regulate *SULT1E1* promoter via the 22 bp enhancer, HNF4α and Δ-1081 *SULT1E1*-Luc or mutated Δ-1081 *SULT1E1*-Luc were cotransfected with RORα WT, RORα S100A (non-phosphorylatable mutant) or RORα S100D (phosphomimetic mutant) into Huh7 cells, respectively. *SULT1E1* promoter activity was significantly repressed by RORα WT and RORα S100A, whereas RORα S100D did not affect promoter activity, and HNF4α greatly activated it (Figure 3B). Intriguingly, HNF4α together with RORα WT or RORα S100A dramatically repressed *SULT1E1* promoter activity, while HNF4α along with RORα S100D significantly activated it (Figure 3B). The mutation of the 22 bp enhancer on the *SULT1E1* promoter remarkably lost its activity and abolished its responsiveness to both HNF4α and RORα in Huh7 cells (Figure 3B). These observations, together with the data shown in Figure 2, indicated that RORα interacting with HNF4α co-repress *SULT1E1* transcription, while phosphorylated RORα at Ser100 interacts with HNF4α to co-activate its expression via the enhancer. The roles of HNF4α and RORα in regulating endogenous *SULT1E1* transcription were further demonstrated by siRNA knockdown experiments in Huh7 cells (Supplementary Figure S2). Additionally, RORα S100D overexpression activated the endogenous *SULT1E1* transcription in HepG2 cell, further demonstrating that phosphorylated RORα and HNF4α activate the promoter in human liver cells (Supplementary Figure S3).

Glucose responsive bindings of HNF4α and RORα to the *SULT1E1* gene

Subsequently, ChIP assays were conducted to examine whether HNF4α and RORα are responsive to glucose exposures and bind the *SULT1E1* enhancer in human liver cells. The anti-phosphor Ser100 RORα antibody was applied to detect whether the conserved phosphorylation site becomes a regulatory factor for *SULT1E1* gene expression in response to glucose exposures. In HepG2 cells, binding of HNF4α to the *SULT1E1* enhancer was slightly weaker under low glucose conditions than it was with high glucose conditions, suggesting that HNF4α may interact with different factors binding to the enhancer at both low glucose and high glucose conditions (Figure 4A). In RORα ectopically expressed HepG2 cells, RORα weakly bound to the *SULT1E1* enhancer in low glucose conditions, whereas phosphorylated RORα was significantly enriched on it at high glucose conditions (Figure 4B). Moreover, the phosphorylation of RORα at Ser100 was induced in high glucose treated HepG2 cells (Figure 4C). In agreement with the results shown in Figures 2 and 3, RORα together with HNF4α suppresses the *SULT1E1* promoter while phosphorylated RORα and HNF4α activate its expression. We hypothesize that RORα interacting with HNF4α binds *SULT1E1* gene to co-repress its expression at low glucose conditions. In response to high glucose signal, RORα is phosphorylated at Ser100, interacting with HNF4α to co-activate *SULT1E1* transcription. The phosphorylation of Ser100 on RORα may be a key factor to regulate *SULT1E1* in response to glucose exposures.

RORα forms a complex with HNF4α binding to the *SULT1E1* gene

A series of CoIP and gel shift assays were deployed to illustrate the interactions between RORα and HNF4α on the *SULT1E1* enhancer. First, CoIP assays showed that HNF4α strongly interacted with RORα regardless of its phosphorylation on Ser100 (Figure 5A), which is consistent with previous observations that HNF4α interacts with RORα to bind the DR1 and RORE overlapping enhancer on the *SULT1E1* gene (Figures 2–4). Incubating the DR1 and RORE probe with a HepG2 nuclear extract resulted in the formation of two equal complexes (Figure 5B, lane 1). An anti-HNF4α antibody shifted the HNF4α complex but not the RORα complex (Figure 5B, lane 2), while both complexes were shifted by an anti-RORα antibody (Figure 5B, lane 3). This confirmed that RORα forms a complex with HNF4α to bind the enhancer and RORα itself binds to the enhancer as well. The interaction between RORα and HNF4α was further demonstrated by using *in vitro* translated proteins in gel shift assays (Supplementary Figure S4). Interestingly, the anti-phosphor Ser100 RORα antibody specifically shifted the HNF4α/RORα complex but not the RORα complex (Figure 5B, lane 7), suggesting that phosphorylated RORα formed a complex with HNF4α binding to *SULT1E1* enhancer. The specificity of this binding was demonstrated by incubating the consensus RORE probe with a HepG2 nuclear extract and respective antibodies (Figure 5B, lane 8–12). These observations are consistent with previous results that phosphorylated RORα forms a complex with HNF4α to bind the *SULT1E1* enhancer at high glucose conditions.

Biochemical Journal (2020) **477** 3583–3598
https://doi.org/10.1042/BCJ20200427

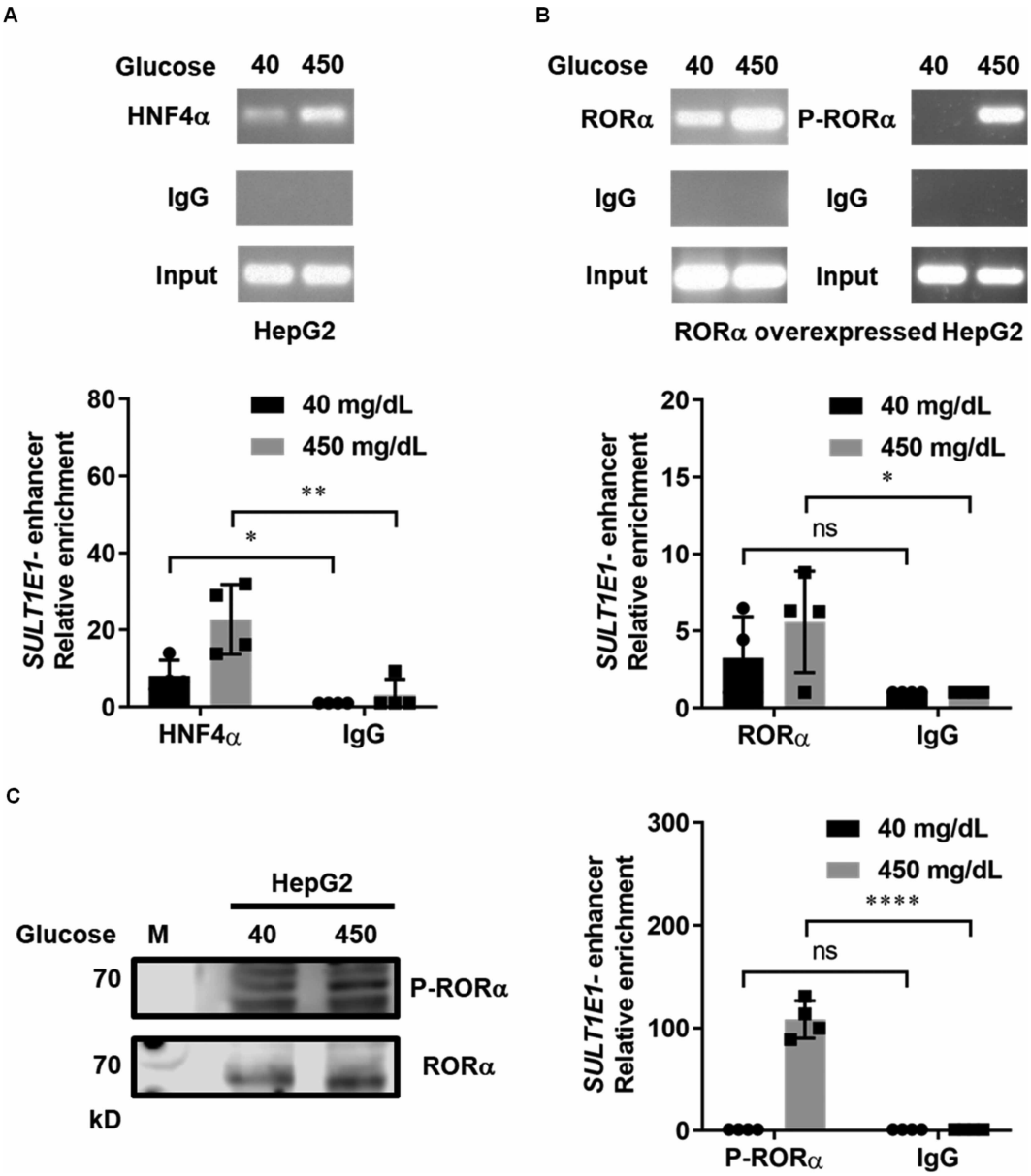

Figure 4. Glucose responsive RORα and HNF4α bindings to the *SULT1E1* enhancer.

(**A**) HepG2 cells or (**B**) RORα overexpressed HepG2 cells were exposed to low glucose or high glucose medium, respectively for 48 h, followed by chromatin immunoprecipitations. The antibodies against HNF4α, RORα and phosphorylated RORα were used to precipitate protein/chromatin binding complexes from the treated cells. The precipitated chromatins were subjected to both real-time PCR and qRT-PCR analysis with a specific primer set (Supplementary Table S2) amplifying the *SULT1E1* enhancer region. A normal IgG was served as a negative control in the assays. The values ($N = 4$) represent means ± S.D. Mean difference is significant from IgG group at **** $P < 0.0001$; ** $P < 0.005$ * $P < 0.05$; ns: non-significant (Student's *t*-test).
(**C**) Phosphorylated RORα expression in response to glucose exposures was detected in HepG2 cells by western blotting with anti-phosphor Ser100 RORα antibody. Non-phosphorylated RORα was served as a loading control.

Casein kinase 1α phosphorylates RORα at Ser100 on *SULT1E1* enhancer

An emerging question as to how casein kinase may mediate RORα phosphorylation at Ser100 in response to high glucose signal was then raised. To address this question, four times repeated DR1 and RORE overlapping enhancer was used as bait to enrich the binding complexes from the low glucose cultured and high glucose

Biochemical Journal (2020) **477** 3583–3598
https://doi.org/10.1042/BCJ20200427

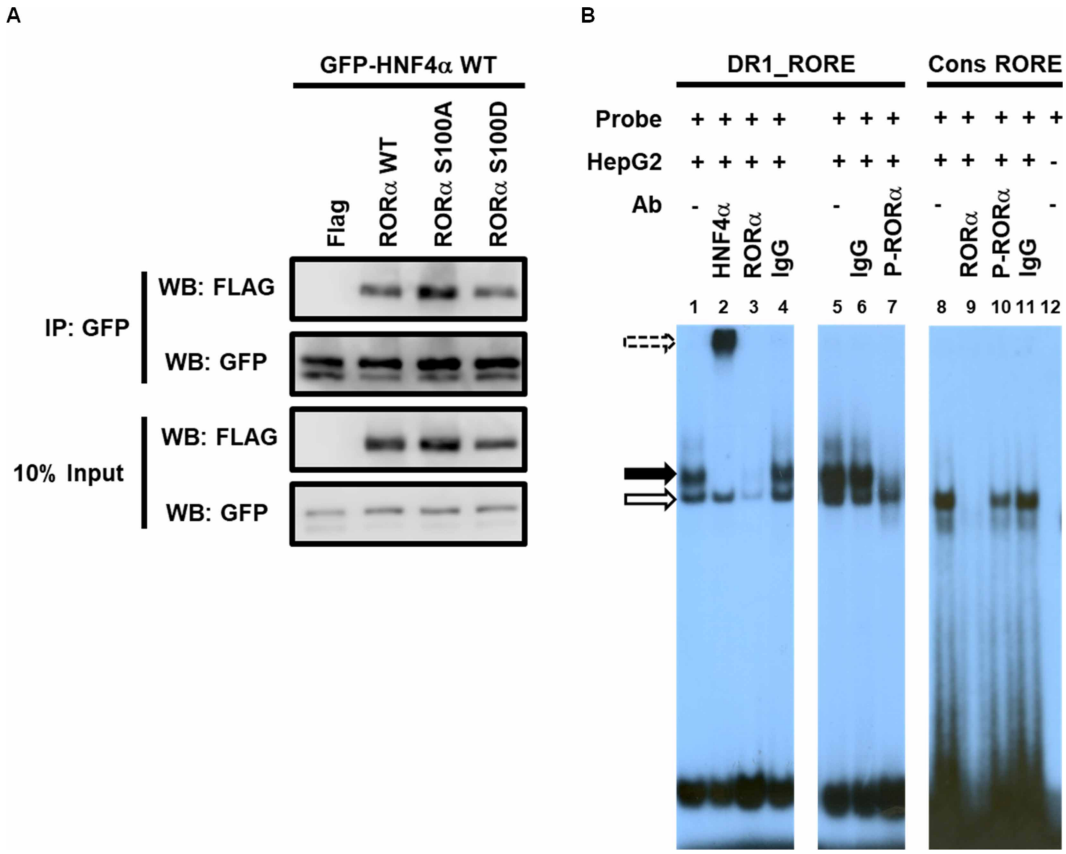

Figure 5. Characterization of RORα/HNF4α binding complexes on the *SULT1E1* enhancer.

(**A**) Physical interaction between HNF4α and RORα. GFP-tagged HNF4α was cotransfected with Flag-tagged RORα WT, RORα S100A or RORα S100D into Cos-1 cells, respectively for 24 h, followed by CoIP reactions with their nuclear extracts. An anti-GFP antibody was used to precipitate GFP-tagged proteins and an anti-Flag antibody was used to detect the proteins that interacted with GFP-tagged HNF4α by western blotting. (**B**) EMSA assays detected the HNF4α and RORα binding complexes on the *SULT1E1* enhancer. The *SULT1E1* DR1_RORE was radioactively labeled, which was incubated with a HepG2 nuclear extract. The antibodies against HNF4α, RORα and phosphorylated RORα at Ser100 were used to supershift (dashed arrow) the formed protein/DNA binding complexes (solid and blank arrows), respectively. A normal IgG was used as a negative control for the used antibodies. The Cons RORE was served as a control to indicate specific interaction between phosphorylated RORα and HNF4α on *SULT1E1* enhancer. Experiments were conducted in triplicates.

cultured HepG2 cell nuclear extracts, respectively. The enriched complexes on the DR1 and RORE overlapping region were then subjected to mass spectroscopic analysis, from which the enriched kinases were listed in Figure 6A. A complete list of enriched factors was submitted to the ProteomeXchange with identifier PXD016385. A ratio (Low/High) between numbers of peptides detected at low glucose and numbers of peptides detected at high glucose was calculated and subjected to Log_2(Low/High) analysis. Of note, the casein kinase 1α (CK1α) and protein kinase C-binding protein 1 (RACK7) were significantly enriched at high glucose condition compared with low glucose condition (Figure 6A).

To test whether CK1α and RACK7 affect the binding of RORα to the *SULT1E1* RORE, gel shift assays were applied by incubating the RORE probe with a HepG2 nuclear extract and respective antibodies. The anti-CK1α antibody significantly blocked the binding of RORα to the RORE (Figure 6B, lane 3), whereas the anti-RACK7 and normal lgG did not affect binding (Figure 6B, lanes 4–5), suggesting an interaction between CK1α and RORα on the enhancer. The specificity of this interaction was illustrated by incubating the consensus RORE with a HepG2 nuclear extract and respective antibodies (Figure 6B, lane 6–10). To further investigate if CK1α mediates RORα phosphorylation at Ser100, *in vitro* phosphorylation assays were performed. First, sequence

Biochemical Journal (2020) **477** 3583–3598
https://doi.org/10.1042/BCJ20200427

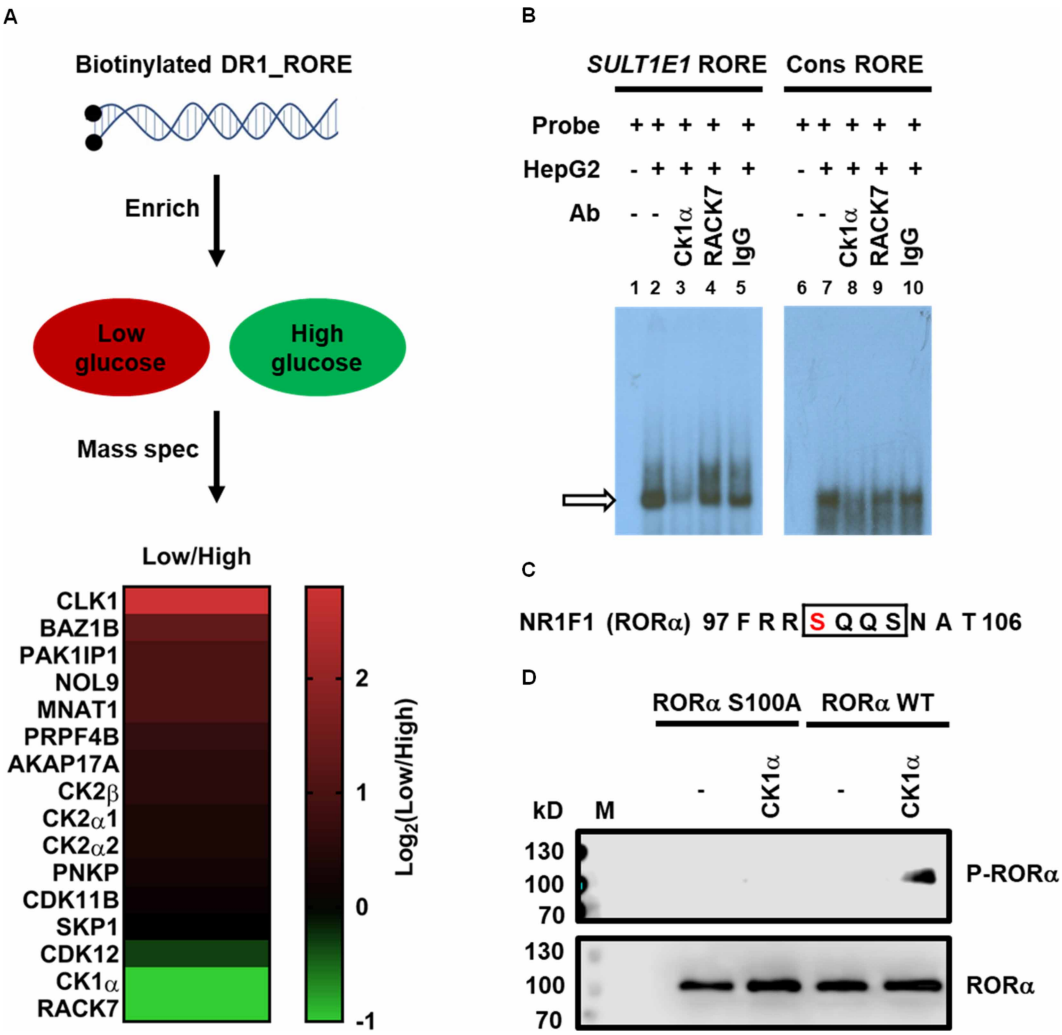

Figure 6. DNA enrichment mass spectrometry detects CK1α to phosphorylate RORα at Ser100.

(**A**) DNA enrichment mass spectrometry analysis. Biotinylated 4 × DR1_RORE of the *SULT1E1* enhancer was incubated with low glucose or high glucose medium treated HepG2 cell nuclear extract, respectively. The enriched binding complexes on the *SULT1E1* enhancer were subjected to quantitative mass spectrometry analysis. A ratio (Low/High) between numbers of peptides detected from low glucose group and numbers of peptides detected from high glucose group was calculated and subjected to Log_2(Low/High) analysis. The enriched kinases were listed on a heat map. (**B**) EMSA assays reveal the binding of CK1α to the RORα on *SULT1E1* enhancer. Radioactive labeled *SULT1E1* RORE was incubated with a HepG2 nuclear extract and respective antibodies. Consensus RORE was served as a positive control. The formed RORα/DNA binding complex was indicated by a blank arrow. (**C**) The Ser100 of RORα (red letter) is a conserved phosphorylation site within a perfect consensus CK1α phosphorylation motif (S/T-X-X-S/T, rectangle). (**D**) RORα was phosphorylated at Ser100 by CK1α. GST-hRORα S100A and GST-hRORα WT were incubated with or without GST-CK1α in kinase buffer containing ATP, respectively, followed by western blotting analysis with the antibodies against phosphorylated RORα and RORα, respectively. Experiments were repeated three times.

analysis of RORα unveiled a consensus CK1α phosphorylation motif on RORα (Figure 6C, rectangle) whose conserved phosphorylation site (Ser100 of RORα) is within the motif [22]. Incubating RORα WT or non-phosphorylatable RORα S100A mutant with or without CK1α, followed by western blotting with an antibody against phosphorylated RORα at Ser100 showed that the RORα WT but not RORα S100A was phosphorylated by CK1α (Figure 6D). These observations illustrate that CK1α phosphorylates RORα at Ser100 on *SULT1E1* enhancer at high glucose conditions.

Biochemical Journal (2020) **477** 3583–3598
https://doi.org/10.1042/BCJ20200427

SULT1E1 enhancer loops its promoter to regulate gene expression

Chromatin conformation capture (3C) assays were applied to detect the chromatin structure of the *SULT1E1* promoter in response to glucose exposures. HepG2 cells were treated by low glucose or high glucose DMEM for 48 h, respectively, followed by chromatin DNA cross-linking and BstYI restriction enzyme digestion. *SULT1E1* promoter was cut at two restriction sites, −1832 bp and +39 bp from the transcription start site, respectively (Figure 7A).

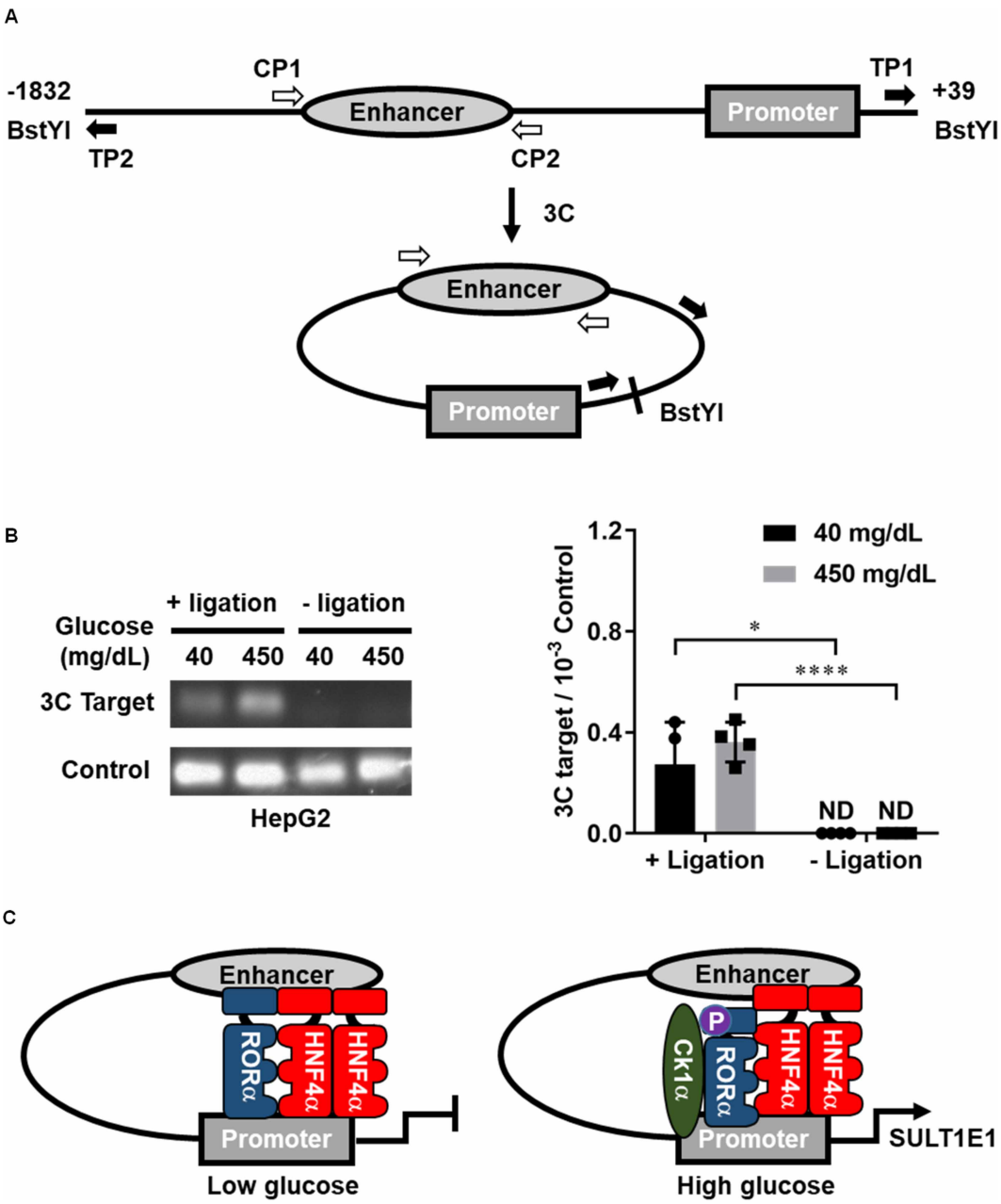

Figure 7. *SULT1E1* chromatin structures in response to glucose signals.

(**A**) Schematic diagram of 3C assay ligated position and primer positions on the *SULT1E1* gene. A 125 bp control product was amplified by using the primers CP1 and CP2 (blank arrows) and a 138 bp ligated product was amplified by using the primers TP1 and TP2 (solid arrows). (**B**) HepG2 cells were treated by low glucose or high glucose DMEM for 48 h, respectively, followed by fixations and BstYI restriction enzyme digestions. After + ligation or — ligation, the 3C ligated product and the control product were detected by real-time PCR and qRT-PCR, respectively. The values ($N = 4$) represent means ± S.D. Mean difference is significant from — ligation group at **** $P < 0.0001$; * $P < 0.05$ (Student's *t*-test). (**C**) A model of glucose responsive *SULT1E1* gene regulation.

After ligation, the ligated point was checked by the primer set (TP1 and TP2, indicated by solid arrows) that amplifies a 138 bp DNA fragment by PCR. Another primer set (CP1 and CP2, indicated by blank arrows) that amplifies a 125 bp *SULT1E1* enhancer fragment was used as loading control primers (Figure 7A). As expected, the *SULT1E1* enhancer appeared to be looped to its promoter as a 138 bp DNA fragment was amplified by RT-PCR after ligation. However, the looped chromatin conformation of the *SULT1E1* gene in HepG2 cells was not affected by the glucose exposures (Figure 7B). The sequences of the ligated fragment were then confirmed by DNA sequencing, from which the joint point was shown in Supplementary Figure S5A. A non-coding region (from +7066 bp to +8570 bp) of the *SULT1E1* gene that has a similar size to the *SULT1E1* promoter was also cut by BstY1 and used as a negative control in the assays. The primer set (TP3 and TP4, indicated by solid arrows) did not amplify any fragments by RT-PCR before or after ligation (Supplementary Figure S5B). The efficacy of these primer sets was validated by RT-PCR using purified fragments (3C target and control) and synthetic DNA (non-3C target) as templates (Supplementary Figure S5C). These results suggested that RORα and HNF4α remained on *SULT1E1* promoter regardless of glucose exposures. High glucose signal stimulated RORα phosphorylation at Ser100 by CK1α, co-activating HNF4α to activate *SULT1E1* transcription (Figure 7C).

Discussion

The liver produces and supplies glucose to peripheral tissues. Unregulated over-production causes diseases such as diabetes and the development of diabetes-related complications including chronic organ inflammation [23]. Various endobiotics modulate these disease states, one of which is estrogen. Postmenopausal women have significantly elevated blood glucose levels, insulin resistance as well as increased circulating inflammatory cytokines, compared with premenopausal women [24–26]. Moreover, E2 administrations improved those diagnoses of postmenopausal women with diabetes [27]. In both male and ovariectomized female mice, estrogen treatment restored insulin action and glucose tolerance [28,29]. In mice fed with high-fat diets, estrogen treatment decreased hepatic expression of glucose-6-phosphatase, lipogenic genes and fasting blood glucose [30]. For these estrogen regulations, SULT1E1 may play a critical role in glucose signaling by metabolically inactivating estrogen in the liver. In fact, hepatic SULT1E1 is induced in high plasma glucose conditions of various mouse models [4,7,31]. Our microarray data revealed that glucose exposures have significantly altered xenobiotic metabolism transcript levels in HepG2 cells (Supplementary Table S1). *Sult1e1* KO mice were utilized to demonstrate that its absence worsened diabetic inflammation to develop sepsis and hepatic ischemia-reperfusion injury [7–9,32].

High glucose induces SULT1E1 expression by activating the *SULT1E1* gene in HepG2 cells. A 22 bp DNA sequence overlapping DR1 and RORE is characterized as the distal enhancer to which HNF4α and RORα bind, respectively, regulating the *SULT1E1* promoter. Phosphorylation of RORα at Ser100 is found to be the glucose response regulator of the transcription. Non-phosphorylated RORα bound RORE interacts with HNF4α on the DR1, which co-represses the *SULT1E1* promoter in low glucose conditions. In response to high glucose, RORα becomes phosphorylated at Ser100 by CK1α, converting its function to co-activate the promoter. During these conversions and co-activation, both RORα and HNF4α remain on the enhancer and keep them in a looping structure with the proximal promoter (Figure 7C). This phosphorylation-mediated mechanism provides us with insights into understanding how two nuclear receptors communicate to regulate hepatic SULT1E1 expression in prenatal livers as well as in diseases and drug treatments of humans.

SULT1E1 is repressed in the liver of adult mice and humans [4,10]. Up-regulation of hepatic SULT1E1 expression in liver-specific HNF4α KO mice suggests that the *Sult1e1* gene is repressed by HNF4α [33]. The molecular mechanism that regulates this repression remains un-investigated. Consistient with previous observations in human fetal livers [11], the *SULT1E1* gene is activated in HepG2 cells in high glucose medium, but is repressed in low glucose medium. HNF4α is found to function as both a transcription activator and repressor, and RORα is characterized as a glucose response regulator of this HNF4α function. Phosphorylated RORα is a glucose response co-activator that binds HNF4α to activate the enhancer. In low glucose medium, RORα is dephosphorylated to bind and co-repress HNF4α. Thus, RORα converts its function from a high glucose response co-activator to a low-glucose response co-repressor through phosphorylation-dephosphorylation of Ser100. Previous studies also showed that an activation function of HNF4α can be repressed. The antibiotic rifampicin activates nuclear receptor PXR which binds HNF4α and dissociates HNF4α from the *SULT1E1* promoter and represses its activity [6]. In other cases, ligand-activated nuclear receptor FXR suppressed the *SULT1E1* promoter by binding PGC1α and preventing it to co-activate HNF4α [12]. Bile acid activated FXR was also found to restrain HNF4α driven *SULT1E1* gene expression through the competitive binding of protein

Biochemical Journal (2020) **477** 3583–3598
https://doi.org/10.1042/BCJ20200427

acetylase-CREB binding protein to the HNF4α, decreasing HNF4α acetylation and nuclear retention [16]. In these types of ligand-dependent repressions, PXR and FXR execute a single function which is to remove the activation activity of HNF4α. On the other hand, RORα plays the dual role of regulating HNF4α to which RORα remains bound, and to either co-activate or co-repress it through phosphorylation.

CK1α is now purified by 22 bp DNA from the *SULT1E1* enhancer-affinity chromatography and is identified by mass spectrometry. RORα's Ser100 constitutes a perfect consensus motif (S/T-X-X-S/T), and is phosphorylated by CK1α in *in vitro* kinase assays. CK1α forms a complex with RORα on the *SULT1E1* promoter, which results in the phosphorylation of Ser100 in response to high glucose. Apparently, CK1α is the kinase that transduces this glucose signal to RORα in HepG2 cells. Previously, yeast casein kinase 1α (YCK1α) was reported to be a down-stream target kinase of glucose signaling that regulates glucose transport and metabolism in yeast cells [34]. The function of casein kinases as glucose signal transducers appears to be conserved cross-species. CK1α is a member of the casein kinase superfamily. Vaccinia virus-related kinase 1 (VRK1), which also belongs to this family, transduced the glucose signal to phosphorylate PXR at Ser350 within the ligand binding domain to regulate gluconeogenesis in HepG2 cells [35]. Recently, we have identified the amino acid residue phosphorylated to activate VRK1 down-stream kinases in response to high glucose in HepG2 cells and phosphorylated VRK1 (manuscript in preparation). VRK1 was also reported to phosphorylate FXR at Ser154 in response to a ligand activation in HepG2 cells [17]; Ser154 resides within the DBD and corresponds to Ser100 of RORα. Casein kinases such as CK1α and VRK1 may be positioned at critical steps of glucose signaling and conserved during evolution. Phenobarbital (PB), a sedative widely used to treat epileptic patients, activates the *Sult1e1* gene transcription in mouse liver [5]. As observed with RORα in HepG2 cells, RORα also repressed the *Sult1e1* gene in mouse liver and, following PB treatment, was phosphorylated at Ser100 to co-activate the CAR-mediated transcription of this gene [5]. Phosphorylation of Ser100 is utilized as a common target of both PB and glucose to transduce their signals to RORα. Future investigations may establish CK1α and/or VRK1 as signal transducers that respond to not only glucose and PB but also various other endogenous and exogenous stimuli.

RORα phosphorylated at Ser100 interacted with HNF4α and converted it to a co-activator. Ser100 is conserved as a phosphorylation motif in 41 out of the total 46 human nuclear receptors and their mouse counterparts [36]. Phosphorylation of this motif and its regulation and regulatory function were first confirmed with CAR at Thr38 in the liver [37]. Phosphorylation of Thr38 represses CAR's constitutive activity and retains CAR in the cytoplasm, conferring CAR with the capability to be activated via dephosphorylation. Subsequently, in addition to RORα, FXR, RXRα and ERα were found to be phosphorylated at their motifs [17,38–40]. Phosphorylated ERα is expressed in neutrophils infiltrating into the mouse uterus and provides neutrophils with migration capability [38]. RXRα is phosphorylated at Thr167 in mouse fat tissues. Our study with RXRα T167A KI mice demonstrated that this phosphorylation regulates energy metabolism in fat tissue and blood glucose levels [39]. Based on these observations, it may be that this conserved phosphorylation functions as a common regulator for nuclear receptors to gain their functional specificities.

The *Sult1e1* was activated in response to phenobarbital-treated or diabetic mouse livers, in which RORα was shown to be phosphorylated at Ser100 to regulate this activation [5,40]. In addition to these drug and pathophysiological responses, the *Sult1e1* gene undergoes multiple and complex expressions, one of which is sexually dimorphic regulation in the liver [41]. However, the lack of proper cell models that conserve this phenotype prevented us to investigate whether phosphorylated RORα regulated sexually dimorphic expressions of the *Sult1e1* gene. HepG2 cells allowed us to specifically examine the glucose responsive regulation without any involvement of hormones such as insulin, glucagon and glucocorticoid [35]. On the other hand, obtained findings were not directly implicated to this regulation in the livers until proper animal models are developed in the future.

In conclusion, we determined the glucose response mechanism by which nuclear receptors RORα and HNF4α communicate to activate the *SULT1E1* gene transcription in HepG2 cells. In response to high glucose, CK1α phosphorylates RORα at Ser100 on the *SULT1E1* promoter. Subsequently, phosphorylated RORα co-activates HNF4α and, thereby, the promoter. In low glucose, RORα was dephosphorylated and co-represses HNF4α. Thus, this phosphorylation serves as a glucose response 'switch' to transduce a glucose signal. Ser100 of RORα is conserved in the majority of mouse and human nuclear receptors. Future studies may characterize CK1α, as a glucose sensor, targeting the corresponding residue of numerous nuclear receptors to integrate their functions in both physiology and pathophysiology, such as in fetal livers and diabetes.

Competing Interests
The authors declare that there are no competing interests associated with the manuscript.

Funding
This work was supported by National Institutes of Health intramural research program Z01ES1005-01.

Author Contributions
H.H. and M.N. designed the experiments and wrote the article. H.H. conducted the experiments and analyzed the data.

Data Availability
The mass spectrometry proteomics data have been deposited to the ProteomeXchange Consortium via the PRIDE partner repository with the dataset identifier PXD016385. The microarray data have been uploaded to the GEO [42] with accession number: GSE140867. All data set generated in the current study will be made to the research community upon requests.

Acknowledgements
We thank Dr. Jason G. Williams from the Mass Spectrometry Research and Support Group of NIEHS for the quantitative mass spectrometry analysis and Dr. Kevin Gerrish from the Molecular Genomics Core Laboratory of NIEHS for microarray analysis. This work was supported by National Institutes of Health intramural research program Z01ES1005-01.

Abbreviations
ANOVA, analysis of variance; CAR, constitutive active/androstane receptor; FXR, farnesoid X receptor; PAPS, phosphor-adenosine phosphosulfate; PB, phenobarbital; PXR, pregnane X receptor; QIAGEN, QIAquick gel extraction kit; STS, steroid sulfatase; SULT1E1, sulfotransferase; VRK1, Vaccinia virus-related kinase 1.

References
1 Falany, C.N., Wheeler, J., Oh, T.S. and Falany, J.L. (1994) Steroid sulfation by expressed human cytosolic sulfotransferases. *J. Steroid Biochem. Mol. Biol.* **48**, 369–375 https://doi.org/10.1016/0960-0760(94)90077-9
2 Negishi, M., Pedersen, L.G., Petrotchenko, E., Shevtsov, S., Gorokhov, A., Kakuta, Y. et al. (2001) Structure and function of sulfotransferases. *Arch. Biochem. Biophys.* **390**, 149–157 https://doi.org/10.1006/abbi.2001.2368
3 Kodama, S. and Negishi, M. (2013) Sulfotransferase genes: regulation by nuclear receptors in response to xeno/endo-biotics. *Drug Metab. Rev.* **45**, 441–449 https://doi.org/10.3109/03602532.2013.835630
4 Song, W.C., Moore, R., McLachlan, J.A. and Negishi, M. (1995) Molecular characterization of a testis-specific estrogen sulfotransferase and aberrant liver expression in obese and diabetogenic C57BL/KsJ-db/db mice. *Endocrinology* **136**, 2477–2484 https://doi.org/10.1210/endo.136.6.7750469
5 Fashe, M., Hashiguchi, T., Yi, M., Moore, R. and Negishi, M. (2018) Phenobarbital induced phosphorylation converts nuclear receptor RORα from a repressor to an activator of the estrogen sulfotransferase gene Sult1e1 in mouse livers. *FEBS Lett.* **592**, 2760–2768 https://doi.org/10.1002/1873-3468.13199
6 Kodama, S., Hosseinpour, F., Goldstein, J.A. and Negishi, M. (2011) Liganded pregnane X receptor represses the human sulfotransferase SULT1E1 promoter through disrupting its chromatin structure. *Nucleic Acids Res.* **39**, 8392–8403 https://doi.org/10.1093/nar/gkr458
7 Gao, J., He, J., Shi, X., Stefanovic-Racic, M., Xu, M., O'Doherty, R.M. et al. (2012) Sex-specific effect of estrogen sulfotransferase on mouse models of type 2 diabetes. *Diabetes* **61**, 1543–1551 https://doi.org/10.2337/db11-1152
8 Chai, X., Guo, Y., Jiang, M., Hu, B., Li, Z., Fan, J. et al. (2015) Oestrogen sulfotransferase ablation sensitizes mice to sepsis. *Nat. Commun.* **6**, 7979 https://doi.org/10.1038/ncomms8979
9 Guo, Y., Hu, B., Huang, H., Tsung, A., Gaikwad, N.W., Xu, M. et al. (2015) Estrogen sulfotransferase is an oxidative stress-responsive gene that gender-specifically affects liver ischemia/reperfusion injury. *J. Biol. Chem.* **290**, 14754–14764 https://doi.org/10.1074/jbc.M115.642124
10 Dubaisi, S., Caruso, J.A., Gaedigk, R., Vyhlidal, C.A., Smith, P.C., Hines, R.N. et al. (2019) Developmental expression of the cytosolic sulfotransferases in human liver. *Drug Metab. Dispos.* **47**, 592–600 https://doi.org/10.1124/dmd.119.086363
11 Dubaisi, S., Barrett, K.G., Fang, H., Guzman-Lepe, J., Soto-Gutierrez, A., Kocarek, T.A. et al. (2018) Regulation of cytosolic sulfotransferases in models of human hepatocyte development. *Drug Metab. Dispos.* **46**, 1146–1156 https://doi.org/10.1124/dmd.118.081398
12 Wang, S., Yuan, X., Lu, D., Guo, L. and Wu, B. (2017) Farnesoid X receptor regulates SULT1E1 expression through inhibition of PGC1α binding to HNF4α. *Biochem. Pharmacol.* **145**, 202–209 https://doi.org/10.1016/j.bcp.2017.08.023
13 Gong, H., Jarzynka, M.J., Cole, T.J., Lee, J.H., Wada, T., Zhang, B. et al. (2008) Glucocorticoids antagonize estrogens by glucocorticoid receptor-mediated activation of estrogen sulfotransferase. *Cancer Res.* **68**, 7386–7393 https://doi.org/10.1158/0008-5472.CAN-08-1545
14 Gong, H., Guo, P., Zhai, Y., Zhou, J., Uppal, H., Jarzynka, M.J. et al. (2007) Estrogen deprivation and inhibition of breast cancer growth in vivo through activation of the orphan nuclear receptor liver X receptor. *Mol. Endocrinol.* **21**, 1781–1790 https://doi.org/10.1210/me.2007-0187
15 Sueyoshi, T., Green, W.D., Vinal, K., Woodrum, T.S., Moore, R. and Negishi, M. (2011) Garlic extract diallyl sulfide (DAS) activates nuclear receptor CAR to induce the Sult1e1 gene in mouse liver. *PLoS ONE* **6**, e21229 https://doi.org/10.1371/journal.pone.0021229

Biochemical Journal (2020) **477** 3583–3598
https://doi.org/10.1042/BCJ20200427

16 Liu, X., Xue, R., Yang, C., Gu, J., Chen, S. and Zhang, S. (2018) Cholestasis-induced bile acid elevates estrogen level via farnesoid X receptor-mediated suppression of the estrogen sulfotransferase SULT1E1. *J. Biol. Chem.* **293**, 12759–12769 https://doi.org/10.1074/jbc.RA118.001789
17 Hashiguchi, T., Arakawa, S., Takahashi, S., Gonzalez, F.J., Sueyoshi, T. and Negishi, M. (2016) Phosphorylation of Farnesoid X receptor at serine 154 links ligand activation With degradation. *Mol. Endocrinol.* **30**, 1070–1080 https://doi.org/10.1210/me.2016-1105
18 Perez-Riverol, Y., Csordas, A., Bai, J., Bernal-Llinares, M., Hewapathirana, S., Kundu, D.J. et al. (2019) The PRIDE database and related tools and resources in 2019: improving support for quantification data. *Nucleic Acids Res.* **47**, D442–Dd50 https://doi.org/10.1093/nar/gky1106
19 Cryer, P.E. (2007) Hypoglycemia, functional brain failure, and brain death. *J. Clin. Invest.* **117**, 868–870 https://doi.org/10.1172/JCI31669
20 American Diabetes Association. (2012) Diagnosis and classification of diabetes mellitus. *Diabetes Care* **35**, S64–S71 https://doi.org/10.2337/dc12-s064
21 Cartharius, K., Frech, K., Grote, K., Klocke, B., Haltmeier, M., Klingenhoff, A. et al. (2005) Matinspector and beyond: promoter analysis based on transcription factor binding sites. *Bioinformatics* **21**, 2933–2942 https://doi.org/10.1093/bioinformatics/bti473
22 Miller, C.J. and Turk, B.E. (2016) Rapid identification of protein kinase phosphorylation site motifs using combinatorial peptide libraries. *Methods Mol. Biol.* **1360**, 203–216 https://doi.org/10.1007/978-1-4939-3073-9_15
23 Gerich, J.E. (1993) Control of glycaemia. *Baillieres Clin. Endocrinol. Metab.* **7**, 551–586 https://doi.org/10.1016/S0950-351X(05)80207-1
24 Carr, M.C. (2003) The emergence of the metabolic syndrome with menopause. *J. Clin. Endocrinol. Metab.* **88**, 2404–2411 https://doi.org/10.1210/jc.2003-030242
25 Pfeilschifter, J., Koditz, R., Pfohl, M. and Schatz, H. (2002) Changes in proinflammatory cytokine activity after menopause. *Endocr. Rev.* **23**, 90–119 https://doi.org/10.1210/edrv.23.1.0456
26 Sites, C.K., Toth, M.J., Cushman, M., L'Hommedieu, G.D., Tchernof, A., Tracy, R.P. et al. (2002) Menopause-related differences in inflammation markers and their relationship to body fat distribution and insulin-stimulated glucose disposal. *Fertil. Steril.* **77**, 128–135 https://doi.org/10.1016/S0015-0282(01)02934-X
27 Salpeter, S.R., Walsh, J.M., Ormiston, T.M., Greyber, E., Buckley, N.S. and Salpeter, E.E. (2006) Meta-analysis: effect of hormone-replacement therapy on components of the metabolic syndrome in postmenopausal women. *Diabetes Obes. Metab.* **8**, 538–554 https://doi.org/10.1111/j.1463-1326.2005.00545.x
28 Stubbins, R.E., Holcomb, V.B., Hong, J. and Nunez, N.P. (2012) Estrogen modulates abdominal adiposity and protects female mice from obesity and impaired glucose tolerance. *Eur. J Nutr.* **51**, 861–870 https://doi.org/10.1007/s00394-011-0266-4
29 Yan, H., Yang, W., Zhou, F., Li, X., Pan, Q., Shen, Z. et al. (2019) Estrogen improves insulin sensitivity and suppresses gluconeogenesis via the transcription factor Foxo1. *Diabetes* **68**, 291–304 https://doi.org/10.2337/db18-0638
30 Bryzgalova, G., Lundholm, L., Portwood, N., Gustafsson, J.A., Khan, A., Efendic, S. et al. (2008) Mechanisms of antidiabetogenic and body weight-lowering effects of estrogen in high-fat diet-fed mice. *Am. J Physiol. Endocrinol. Metab.* **295**, E904–E912 https://doi.org/10.1152/ajpendo.90248.2008
31 Leiter, E.H. and Chapman, H.D. (1994) Obesity-induced diabetes (diabesity) in C57BL/KsJ mice produces aberrant trans-regulation of sex steroid sulfotransferase genes. *J. Clin. Invest.* **93**, 2007–2013 https://doi.org/10.1172/JCI117194
32 Garbacz, W.G., Jiang, M., Xu, M., Yamauchi, J., Dong, H.H. and Xie, W. (2017) Sex- and tissue-specific role of estrogen sulfotransferase in energy homeostasis and insulin sensitivity. *Endocrinology* **158**, 4093–4104 https://doi.org/10.1210/en.2017-00571
33 Lu, H., Gonzalez, F.J. and Klaassen, C. (2010) Alterations in hepatic mRNA expression of phase II enzymes and xenobiotic transporters after targeted disruption of hepatocyte nuclear factor 4 alpha. *Toxicol. Sci.* **118**, 380–390 https://doi.org/10.1093/toxsci/kfq280
34 Snowdon, C. and Johnston, M. (2016) A novel role for yeast casein kinases in glucose sensing and signaling. *Mol. Biol. Cell* **27**, 3369–3375 https://doi.org/10.1091/mbc.E16-05-0342
35 Gotoh, S., Miyauchi, Y., Moore, R. and Negishi, M. (2017) Glucose elicits serine/threonine kinase VRK1 to phosphorylate nuclear pregnane X receptor as a novel hepatic gluconeogenic signal. *Cell. Signal.* **40**, 200–209 https://doi.org/10.1016/j.cellsig.2017.09.003
36 Negishi, M. (2017) Phenobarbital meets phosphorylation of nuclear receptors. *Drug Metab. Dispos.* **45**, 532–539 https://doi.org/10.1124/dmd.116.074872
37 Mutoh, S., Osabe, M., Inoue, K., Moore, R., Pedersen, L., Perera, L. et al. (2009) Dephosphorylation of threonine 38 is required for nuclear translocation and activation of human xenobiotic receptor CAR (NR1I3). *J. Biol. Chem.* **284**, 34785–34792 https://doi.org/10.1074/jbc.M109.048108
38 Shindo, S., Moore, R., Flake, G. and Negishi, M. (2013) Serine 216 phosphorylation of estrogen receptor α in neutrophils: migration and infiltration into the mouse uterus. *PLoS ONE* **8**, e84462 https://doi.org/10.1371/journal.pone.0084462
39 Sueyoshi, T., Sakuma, T., Shindo, S., Fashe, M., Kanayama, T., Ray, M. et al. (2019) A phosphorylation-deficient mutant of retinoid X receptor α at Thr 167 alters fasting response and energy metabolism in mice. *Lab. Invest.* **99**, 1470–1483 https://doi.org/10.1038/s41374-019-0266-1
40 Yi, M., Fashe, M., Arakawa, S., Moore, R., Sueyoshi, T. and Negishi, M. (2020) Nuclear receptor CAR-ERα signaling regulates the estrogen sulfotransferase gene in the liver. *Sci. Rep.* **10**, 5001 https://doi.org/10.1038/s41598-020-61767-9
41 Matsushita, N., Hassanein, M.T., Martinez-Clemente, M., Lazaro, R., French, S.W., Xie, W. et al. (2017) Gender difference in NASH susceptibility: roles of hepatocyte ikkβ and Sult1e1. *PLoS ONE* **12**, e0181052 https://doi.org/10.1371/journal.pone.0181052
42 Barrett, T., Troup, D.B., Wilhite, S.E., Ledoux, P., Evangelista, C., Kim, I.F. et al. (2011) NCBI GEO: archive for functional genomics data sets–10 years on. *Nucleic Acids Res.* **39**, D1005–D1D10 https://doi.org/10.1093/nar/gkq1184

Supplementary Figures Legends

Supplementary Figure 1. High glucose induces SULT1E1 expression in HepG2 3D culture and Huh7 cells. (A) HepG2 3D spheroids and (B) Huh7 cells were treated by low glucose and high glucose DMEM respectively for 48 hours, followed by measuring their *SULT1E1* mRNA expression levels. (D) HepG2 and Huh7 cell viabilities in response to low glucose and high glucose exposures for 48 hours were measured. The values (N = 3) represent means ± S.D. Mean difference is significant from low glucose treated group at ****, $p < 0.0001$; ***, $p < 0.0005$ (Student's *t*-test).

Supplementary Figure 2. HNF4α activates while RORα suppresses *SULT1E1* in Huh7 cells. (A - B) HNF4α was knocked down by siRNA in Huh7 cells, followed by low glucose and high glucose treatments respectively for 48 hours. *SULT1E1* and *HNF4α* mRNA expression levels of these treated cells were subsequently detected. (C - D) RORα was knocked down by siRNA in Huh7 cells, followed by low glucose and high glucose treatments respectively for 48 hours. *SULT1E1* and *RORα* gene expressions of these treated cells were subsequently detected. The values (N = 3) represent means ± S.D. Mean difference is significant from scramble siRNA transfected group ****, $p < 0.0001$; ***, $p < 0.0005$; *, $p < 0.05$ (Student's *t*-test).

Supplementary Figure 3. RORα S100D activates endogenous *SULT1E1* in HepG2 cells. (A) Flag-tagged RORα WT, RORα S100A or RORα S100D was transfected into HepG2 cells respectively for 24 hours, followed by measuring their *SULT1E1* mRNA expression levels. The values (N = 4) represent means ± S.D. Mean difference is significant from empty vector transfected group at ***, $p < 0.0005$ (One-way ANOVA). (B) The expression patterns of these

Flag-tagged RORαs in the nuclei of transfected HepG2 cells were detected by western blotting with an anti-Flag antibody. Nuclear protein HDAC1 was used as a loading control.

Supplementary Figure 4. RORα interacting with HNF4α binds to the *SULT1E1* gene. (A) *In vitro* translated Flag-tagged HNF4α, RORα WT, RORα S100A and RORα S100D were applied in the gel shift assays. The expression levels of these *in vitro* translated proteins were detected by western blotting with an anti-Flag antibody. (B) The radioactive labeled *SULT1E1* DR1_RORE probe was incubated with HNF4α, HNF4α/RORα WT mixture, HNF4α/RORα S100A mixture or HNF4α/RORα S100D mixture respectively. The formed complex (indicated by a solid arrow) was recognized by the antibodies against HNF4α and RORα respectively. Supershifted bands were indicated by a dashed arrow. A normal IgG was used as a control for the antibodies used in the assays. (C) Binding capacities of the *in vitro* translated RORα WT, RORα S100A and RORα S100D to a consensus RORE were tested by gel shift assays.

Supplementary Figure 5. Controls for 3C assays. (A) The 3C target was sequenced, from which the ligated point was displayed. (B) A non-coding region (from +7066 bp to +8570 bp) of the *SULT1E1* gene that has a similar size to the *SULT1E1* promoter was used as a negative control in the 3C assays. Primer set (TP3 and TP4, indicated by solid arrows) was used to amplify a 127 bp non-3C target from the glucose treated HepG2 cells. (C) The efficiency of the primer sets used in the 3C assays was validated by RT-PCR using purified fragments (3C target and Control) and synthesized DNA (Non-3C target) as templates.

Supplementary Table 1. Glucose exposures alter xenobiotic metabolism in HepG2 cells.

Microarray analysis of the glucose treated HepG2 cells. Gene expression analysis was conducted using Agilent Whole Human Genome 4 × 44 Version 2 multiplex format oligo arrays (026652) (Agilent Technologies) following the Agilent 1-color microarray-based gene expression analysis protocol. The values (N = 4) represent means ± S.D. Mean difference between low glucose treated group and high glucose treated group was compared by an ANOVA and Benjamini-Hochberg multiple test correction with a p-value of $p<0.05$. Xenobiotic related genes that have a fold change (high glucose group/low glucose group) more than ±2 were listed in the table. The data sets (accession: GSE140867) are accessible at GEO.

Supplementary Table 2. Primers, oligonucleotides and probes used in the study.

The primers, oligonucleotides and probes used for plasmid constructions, DNA affinity chromatography-mass spectrometry, qRT-PCR, EMSA, ChIP and 3C assays in the study are listed in the table. The mutated sequences are underlined.

Supplementary Figure 1

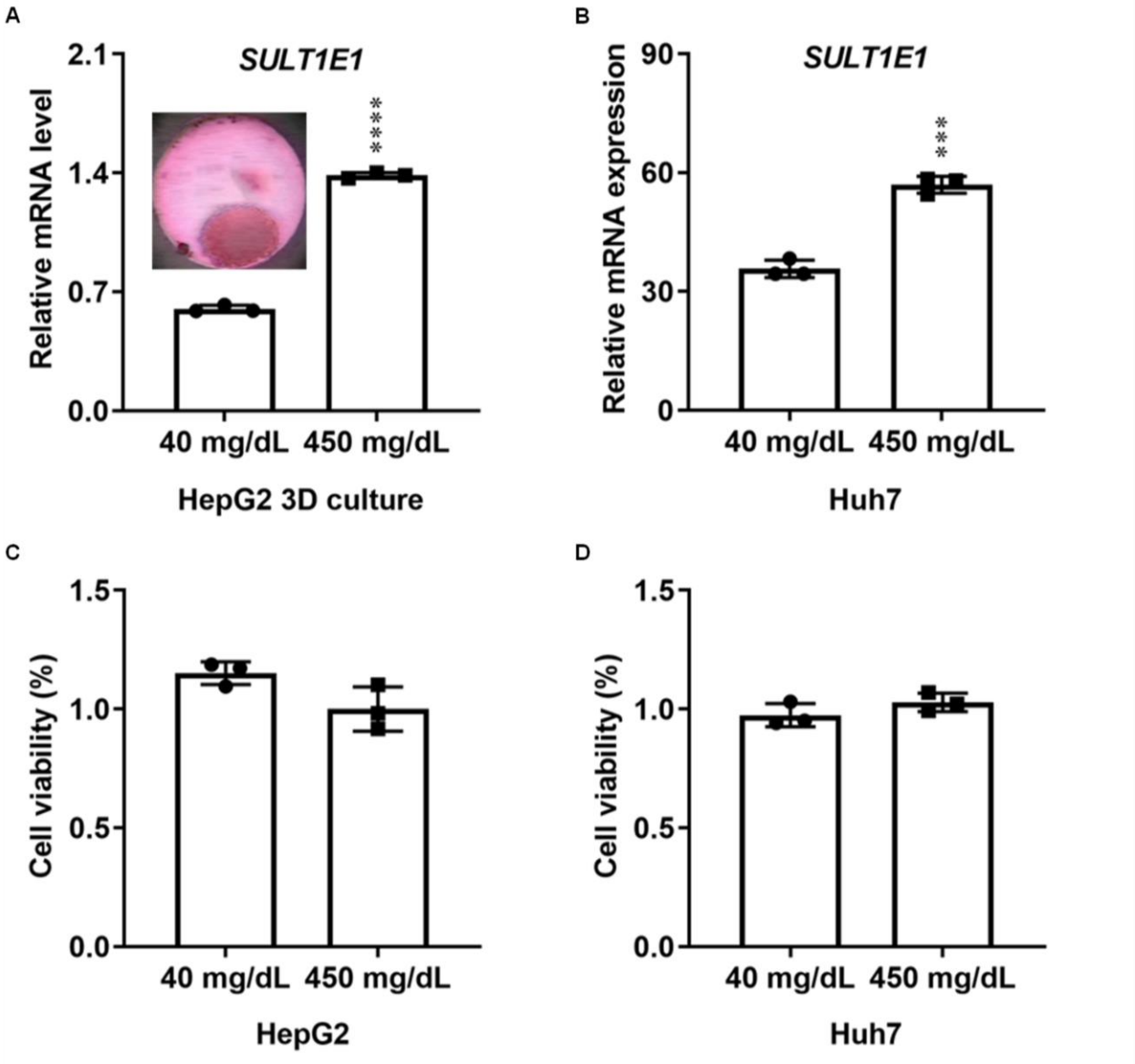

Supplementary Figure 2

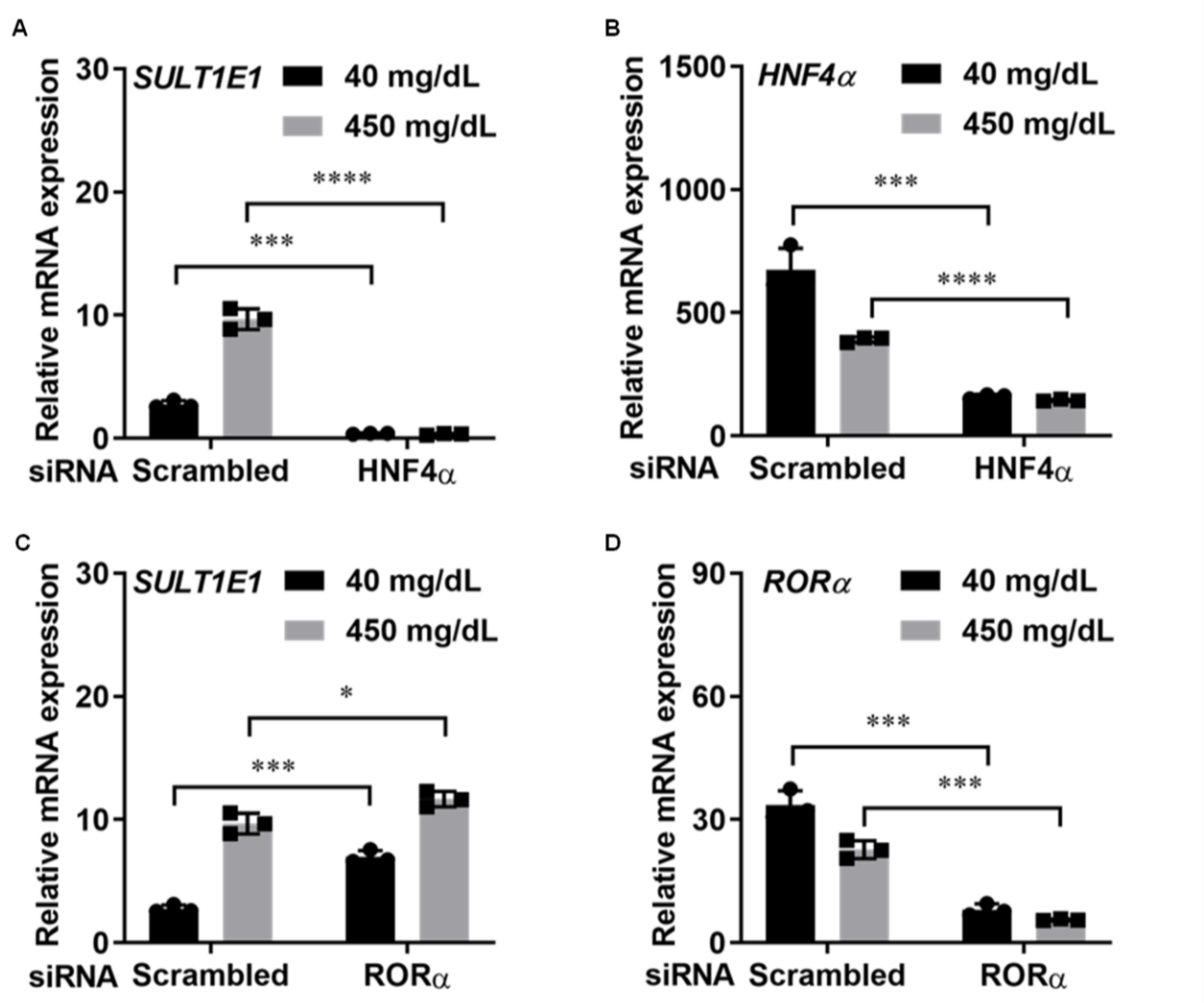

Supplementary Figure 3

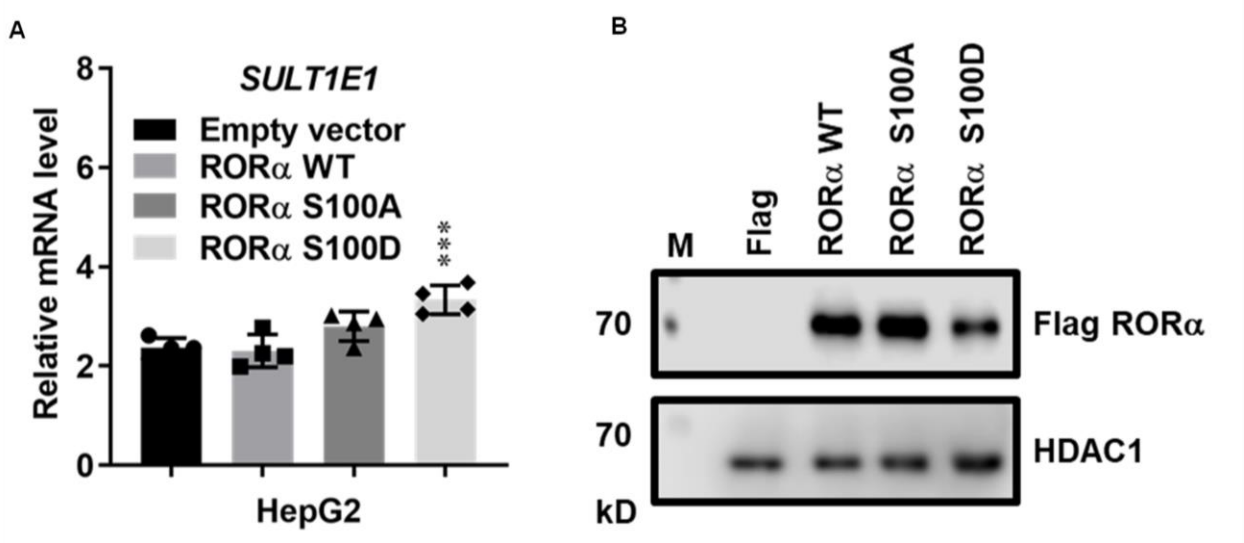

Supplementary Figure 4

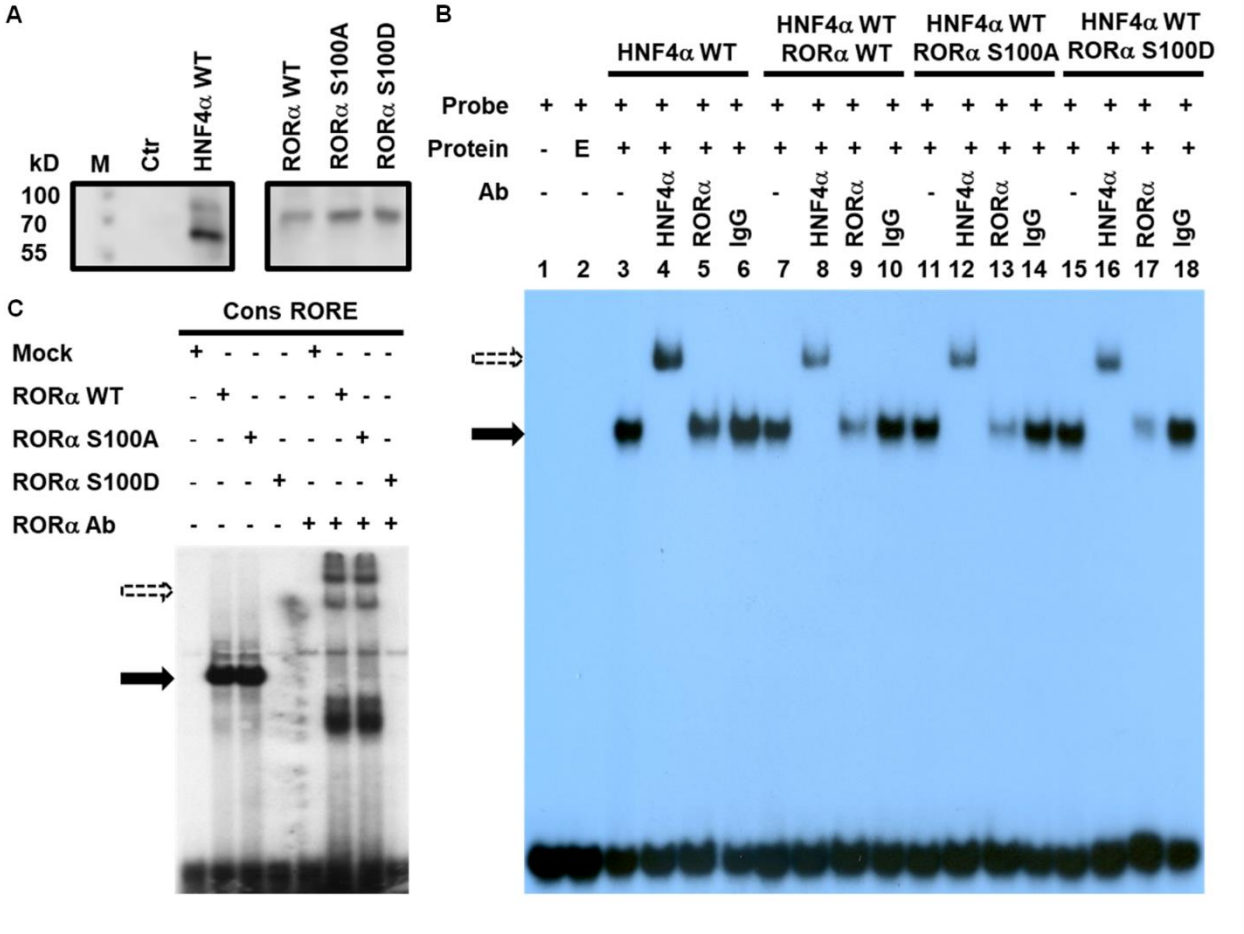

Supplementary Figure 5

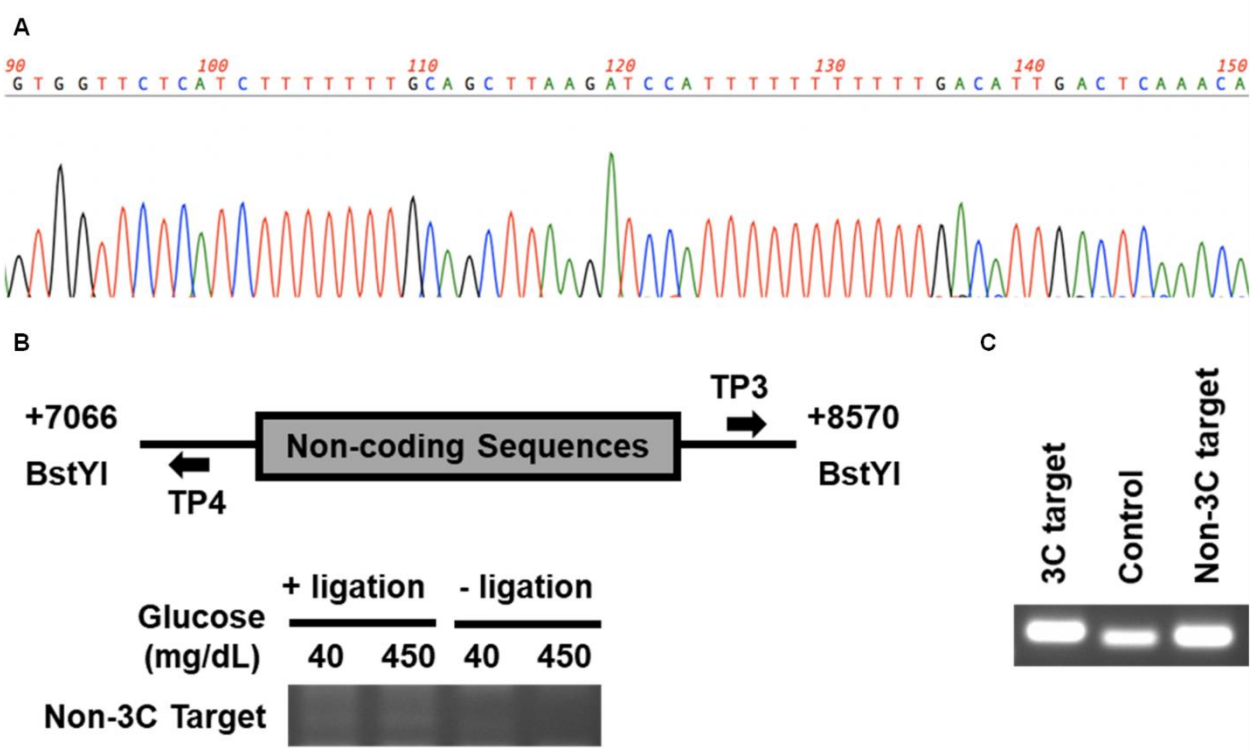

Supplementary Table 1

Name	Fold Change*	p-value
	SULTs	
SULT2A1	9.569	1.19E-12
SULT1E1	7.484	1.26E-05
SULT1B1	2.87	0.032
SULT1C2	2.597	7.53E-07
SULT1C4	-2.1	0.0295
	CYPs	
CYP3A7	3.721	4.87E-09
CYP3A5	2.798	1.69E-05
CYP2D6	2.3407	1.49E-05
CYP2U1	2.3151	5.5645E-06
CYP4F3	2.2599	2.6359E-07
CYP2R1	-2	1.3834E-09
CYP2S1	-3.1089	0.0025
CYP1A1	-4.311	1.84E-09
CYP4F11	-6.4977	1.9544E-11
	UGTs	
UGT2B11	2.843	1.89E-12
UGT2B15	2.595	5.53E-06
UGT2B10	2.419	1.03E-09
UGT2B7	2.29	2.74E-07
	GSTs	
GSTM2	16.404	2.64E-05
GSTM4	5.076	7.74E-09
GSTO2	3.356	1.43E-10
MGST2	2.748	1.22E-12
GSTA4	2.426	2.24E-10
GSTT1	2.343	2.41E-11
GSTK1	2.341	2.24E-09
MGST1	-2.836	2.4E-12
GSTA2	-3.947	5.5E-11
GSTA5	-5.966	2.33E-08

* Fold change represents high glucose group/low glucose group.

Supplementary Table 2

Construction of mutant *SULT1E1* promoters	
Δ-1081 DR1 mutant	5’-TGATTTACAACACAGTAAAATAAATACTAGTTAGGAGAAAGTTTGGGATTTAAAAGTCACTAAGAGAAACATAACATCTACATTAACTATT-3’ 5’-AATAGTTAATGTAGATGTTATGTTTCTCTTAGTGACTTTTAAATCCCAAACTTTCTCCTAACTAGTATTTATTTTACTGTGTTGTAAATCA-3’
Δ-1081 RORE mutant	5’-TGATTTACAACACAGTAAAATAAATACTAGTTAGGAGAAAGTTCAAAGTTTAAGGACTACTAAGAGAAACATAACATCTACATTAACTAT-3’ 5'-ATAGTTAATGTAGATGTTATGTTTCTCTTAGTAGTCCTTAAACTTTGAACTTTCTCCTAACTAGTATTTATTTTACTGTGTTGTAAATCA-3’
Δ-1081 DR1_RORE mutant	5’-ACAGTAAAATAAATACTAGTTAGGAGAAAGTTTGGGATTTAAGGACTACTAAGAGAAACATAACATCTACATTAACTATTGCATC-3’ 5’-GATGCAATAGTTAATGTAGATGTTATGTTTCTCTTAGTAGTCCTTAAATCCCAAACTTTCTCCTAACTAGTATTTATTTTACTGT-3’
Construction of HNF4α expression plasmid	
HNF4α_F	5’-ATCATTAAGCTTATGCGACTCCAAAACCC-3’
HNF4α_R	5’-ATCATTGGATCCCTAGATAACTTCCTGCTTGGTG-3’
Oligonucleotides for DNA affinity chromatography-mass spectrometry	
4×DR1_RORE_F	5’-CTAGGAGAAAGTTCAAAGTTTAAAAGTCACTAAGATAGGAGAAAGTTCAAAGTTTAAAAGTCACTAAGATAGGAGAAAGTTCAAAGTTTAAAAGTCACTAAGAG-3’
4×DR1_RORE_R	5’-GATCCTCTTAGTGACTTTTAAACTTTGAACTTTCTCCTATCTTAGTGACTTTTAAACTTTGAACTTTCTCCTATCTTAGTGACTTTTAAACTTTGAACTTTCTCCTATCTTAGTGACTTTTAAACTTTGAACTTTCTCCTAGGTAC-3’
4×1E1_F	5’-AAGTTGGCCGCAGTGTTATC-3’
4×1E1_R	5’-TGGGCGGGGCCAGATCC-3’
Assay on demand primers	
Human SULT1E1	Hs00193690_m1
Human STS	Hs00996676_m1
Human TFF1	Hs00907239_m1
Human HNF4α	Hs00230853_m1
Human RORα	Hs00536545_m1
Human ACTB	Hs99999903_m1

EMSA probes	
DR1_RORE	5’-GATCTAGGAGAAAGTTCAAAGTTTAAAAGTCACTAAGA-3’ 5’-GATCTCTTAGTGACTTTTAAACTTTGAACTTTCTCCTA-3’
DR1	5’-GATCAGGAGAAAGTTCAAAGTTTAAAA-3’ 5’-GATCTTTTAAACTTTGAACTTTCTCCT-3’
RORE	5’-GATCTCAAAGTTTAAAAGTCACTAAGA-3’ 5’-GATCTCTTAGTGACTTTTAAACTTTGA-3’
Consensus RORE	5’-GATCTCGACTCGTATATCAAGGTCATGCTG-3’ 5’-GATCCAGCATGACCTTGATATACGAGTCGA-3’
ChIP assay primers	
SULT1E1 enhancer_F	5’-AAAGTACTCTGGACAAGCAAAC-3’
SULT1E1 enhancer_R	5’-GAGGCTCACTCTTACAAGACTC-3’
3C assay primers	
Control (CP1)_F	5’-CTCTGGACAAGCAAACATTGA-3’
Control (CP2)_R	5’-CATTTCCTTTGAGAGGCTCACTC-3’
Ligated (TP1)_F	5’-TCACCAGAAACATTCCAAATGCAG-3’
Ligated (TP2)_R	5’-CTGAAACCTCATTCTTCTCCATGA-3’
Ligated (TP3)_F	5’-TGGCTGGGTCAAATGGTATT-3’
Ligated (TP4)_R	5’-GCATGGAATGACTTCAGCAG-3’
Non-3C target template	5’-TGGCTGGGTCAAATGGTATTTCTAGTTCTAGATCTACAGACAA AAATCAAAGATTGCCAGGTTAGTTTGTTTTTATCATTAGCAATCC TAGATAGACGATATACGTCCTGCTGAAGTCATTCCATGC-3’

Mutated sequences are underlined